REMARKS

Claims 12-39 presently appear in this case. Claims 12-16 and 24-39 have been withdrawn from consideration. No claims have been allowed. The official action of June 15, 2005, has now been carefully studied. Reconsideration and allowance are hereby respectfully urged.

Briefly, the present invention relates to an RNA molecule that targets mRNA encoding a polypeptide having the amino acid sequence of SEQ ID NO:10. The targeting preferably prevents processing, splicing, transport, or translation of the mRNA, or results in mRNA degradation. The RNA may be an antisense RNA or a ribozyme. The invention further relates to an RNA molecule that targets DNA encoding a polypeptide having the amino acid sequence of SEQ ID NO:10. Preferably, the targeting results in a transcriptionally inactive product. Applicants also consider therapeutic methods of use of such RNA to be part of the present invention.

The examiner has objected to the disclosure for failing to have a sequence listing that includes the sequences shown in Figure 6B.

At page 8, the specification has now been amended to specify the sequence ID numbers of the sequences shown in Figure 6B. Furthermore, applicants have added into the present specification a new paper copy Sequence Listing section

according to 37 C.F.R. §1.821(c) as new pages 1-22. This new paper copy includes sequences 12 and 13. Furthermore, attached hereto is a 3 1/2" disk containing the "Sequence Listing" in computer readable form in accordance with 37 C.F.R. §1.821(e). The paper and computer readable form are attached hereto as Appendix A. Thus, this objection has been obviated.

The following statement is provided to meet the requirements of 37 C.F.R. §1.821(f) and 1.821(g), §1.825(a) and 1.825(b).

I hereby state, in accordance with 37 C.F.R. §1.825(a), that the amendments included in the substitute sheets of the sequence listing are believed to be supported in the application as filed and that the substitute sheets of the sequence listing are not believed to include new matter.

I hereby further state, in accordance with 37 C.F.R. §1.825(b), that the attached copy of the computer readable form is the same as the attached substitute paper copy of the sequence listing.

Under U.S. rules, each sequence must be classified in <213> as an "Artificial Sequence", a sequence of "Unknown" origin, or a sequence originating in a particular organism, identified by its scientific name.

Neither the rules nor the MPEP clarify the nature of the relationship which must exist between a listed sequence

and an organism for that organism to be identified as the origin of the sequence under <213>.

Hence, counsel may choose to identify a listed sequence as associated with a particular organism even though that sequence does not occur in nature by itself in that organism (it may be, e.g., an epitopic fragment of a naturally occurring protein, or a cDNA of a naturally occurring mRNA, or even a substitution mutant of a naturally occurring sequence). Hence, the identification of an organism in <213> should not be construed as an admission that the sequence *per se* occurs in nature in said organism.

Similarly, designation of a sequence as "artificial" should not be construed as a representation that the sequence has no association with any organism. For example, a primer or probe may be designated as "artificial" even though it is necessarily complementary to some target sequence, which may occur in nature. Or an "artificial" sequence may be a substitution mutant of a natural sequence, or a chimera of two or more natural sequences, or a cDNA (i.e., intron-free sequence) corresponding to an intron-containing gene, or otherwise a fragment of a natural sequence.

The examiner should be able to judge the relationship of the enumerated sequences to natural sequences by giving full consideration to the specification, the art

cited therein, any further art cited in an IDS, and the results of his or her sequence search against a database containing known natural sequences.

Claims 20 and 22 have been rejected under 35 U.S.C. §112, first paragraph, as failing to comply with the written description requirement. The examiner states that claim 20 is drawn to an RNA molecule that targets mRNA encoding a polypeptide having the amino acid sequence of SEQ ID NO:10 that is an antisense RNA molecule, and claim 22 is drawn to an RNA molecule that targets DNA encoding a particular polypeptide. The examiner states that he could find support only for RNA molecules that are ribozymes, but no support could be found for new claims to an RNA molecule that is an antisense RNA, or an RNA molecule that targets DNA. This rejection is respectfully traversed.

The present specification as filed in paragraph [0164] incorporates by reference the full disclosure of each of the publications that have been listed in the specification. Among the references listed on pages 76-87 are the following: Holzmayer et al "Isolation of Dominant Negative Mutants and Inhibitory Antisense RNA Sequences by Expression Selection of Random DNA Fragments", Nucleic Acids Res 20(4):711-717 (1992); and Whitesell et al, "Episome-generated N-*myc* antisense RNA restricts the differentiation

potential of primitive neuroectodermal cell lines", Mol Cell Biol 11:1360-1371 (1991), copies of which are attached hereto. Each of these deal with antisense RNA. Thus, one of ordinary skill in the art reading the present specification would have understood that the reference to antisense oligonucleotides encompasses both antisense DNA and antisense RNA, which were well known at the time of the filing of the present application. That the term "oligonucleotide" as used in the present specification encompasses RNA is apparent from paragraph [0064] of the present specification, which states that the bases of the oligonucleotides of the invention can include uracil.

Page 23 of the present specification, at line 9, in paragraph [0056] has now been amended to specify that isolation of inhibitory antisense RNA is disclosed in Holzmayer (1992), as is apparent from its title. This is not new matter in view of the fact that Holzmayer was fully incorporated by reference into the present specification. Furthermore, at page 25, line 21, in paragraph [0059], the reference to Whitesell et al (1991) was augmented to specify that in that publication the antisense oligonucleotide is antisense RNA, as is apparent from the title. It is believed that these amendments to the specification, which do not comprise new matter in view of the fact that the publications

referred to were incorporated by reference into the specification, provide written description support for claims 20 and 22. Accordingly, this written description rejection of claims 20 and 22 has now been overcome. Reconsideration and withdrawal of this rejection are, therefore, respectfully urged.

Claims 17-20, 22 and 23 have been rejected under 35 U.S.C. §102(e) or 35 U.S.C. §103(a) as being anticipated by or obvious over Chang. The examiner states that Chang discloses an oligonucleotide of SEQ ID NO:15 that is 84.2% identical to the nucleic acid sequence encoding the polypeptide of SEQ ID NO:10, with the 5' end of the 19 nucleobase oligonucleotide of Chang being 100% identical over the first sixteen contiguous nucleobases, to the polypeptide of SEQ ID NO:10 of the instant invention. This rejection is respectfully traversed.

The oligonucleotide of SEQ ID NO:15 of Chang, referred to by the examiner, is a DNA sequence. It includes thiamine and not uracil. As the claims require that the antisense be an RNA molecule and not a DNA molecule, this sequence cannot anticipate. The examiner has not explained why it would be obvious to change the DNA of Chang to an RNA molecule. Accordingly, neither are the present claims obvious from Chang. Reconsideration and withdrawal of this rejection are, therefore, respectfully urged.

Claims 17-20 and 22-23 have been rejected under 35 U.S.C. §102(e) or 35 U.S.C. §103(a) as being anticipated by or obvious over Sutcliffe. The examiner states that Sutcliffe discloses SEQ ID NO:16 that is twenty nucleobases in length, and 100% identical to the nucleic acid sequence encoding the polypeptide of SEQ ID NO:10. This rejection is also respectfully traversed.

SEQ ID NO:16 of Sutcliffe is a DNA sequence. Thus, Sutcliffe cannot anticipate or make obvious the present invention for the same reasons as discussed above with respect to Change. Reconsideration and withdrawal of this rejection are, therefore, also respectfully urged.

Claims 17-23 have been rejected under 35 U.S.C. §102(e) or 35 U.S.C. §103(a) as being anticipated by or obvious over Pavco. The examiner states that Pavco discloses an RNA molecule that is a hammerhead ribozyme of SEQ ID NO:7749, the binding arms of which target (with 94.1% complementarity including the first five nucleobases from the 5' and 3' end of each binding arm, thus indicating that sufficient binding for mRNA degradation would occur by complementary binding of each binding arm), the nucleic acid sequence (the mRNA or the coding DNA) encoding the polypeptide of SEQ ID NO:10 of the instant invention. This rejection is also respectfully traversed.

The target sequence to which the examiner refers is mostly T's and an occasional G. This is a very non-specific sequence with very little complexity and would never be used by anyone of ordinary skill in the art of designing an antisense target. There are at least six different human genes that have 100% complementarity to this 17-nucleotide sequence and several more with slightly shorter than 100% complementarity. Accordingly, this molecule does not target mRNA encoding a polypeptide having the amino acid sequence of SEQ ID NO:10 as those of ordinary skill in the art of antisense technology understand that targeting requires a certain degree of specificity.

Furthermore, applicants have reason to believe that the mRNA ribozyme of Pavco will not bind to SEQ ID NO:10 and cleave it. It is expected that a declaration to this effect will be filed during the three-month suspension period following the filing of the RCE on even date herewith. Accordingly, the present claims are neither anticipated nor made obvious by Pavco. Reconsideration and withdrawal of this rejection are also respectfully urged.

The examiner states that the prior art made of record and not relied upon but considered pertinent to applicants' disclosure that was set forth in the action mailed December 28, 2004, was cited as evidence of a wide variety of

prior art that could be applied against the instant claims but was not so applied in the interest of compact prosecution. The examiner says that there is no implicit or explicit recognition that this prior art was insufficiently pertinent to warrant its application against the claims.

In view of the fact that the rejections of record have been overcome, it is requested that the examiner analyze the remaining art and determine whether or not they are sufficiently pertinent to warrant their application against the claims and, if so, to make such a rejection. Only then can applicants make a reasoned determination whether to continue prosecution of this case.

It is submitted that all of the claims now present in the case clearly define over the references of record and fully comply with 35 U.S.C. §112. Reconsideration and allowance are, therefore, earnestly solicited.

Respectfully submitted,

BROWDY AND NEIMARK, P.L.L.C.
Attorneys for Applicant(s)

By _____
Roger L. Browdy
Registration No. 25,618

RLB:rd
Telephone No.: (202) 628-5197
Facsimile No.: (202) 737-3528
G:\BN\Q\QBI\Einat1.1D\Pto\AmendmentD.doc

Nucleic Acids Research, Vol. 20, No. 4 711–717

Isolation of dominant negative mutants and inhibitory antisense RNA sequences by expression selection of random DNA fragments

Tatyana A.Holzmayer, Dmitry G.Pestov and Igor B.Roninson*
Department of Genetics, University of Illinois at Chicago, 808 South Wood St, Chicago, IL 60612, USA

Received December 3, 1991; Revised and Accepted January 15, 1992

ABSTRACT

Selective inhibition of specific genes can be accomplished using genetic suppressor elements (GSEs) that encode antisense RNA, dominant negative mutant proteins, or other regulatory products. GSEs may correspond to partial sequences of target genes, usually identified by trial and error. We have used bacteriophage lambda as a model system to test a concept that biologically active GSEs may be generated by random DNA fragmentation and identified by expression selection. Fragments from eleven different regions of lambda genome, encoding specific peptides or antisense RNA sequences, rendered *E. coli* resistant to the phage. Analysis of these GSEs revealed some previously unknown functions of phage lambda, including suppression of the cellular lambda receptor by an 'accessory' gene of the phage. The random fragment selection strategy provides a general approach to the generation of efficient GSEs and elucidation of novel gene functions.

INTRODUCTION

Selective suppression of a specific gene represents a general approach to the analysis of gene function. Such suppression can be accomplished either by gene disruption or by introduction of a genetic element that inhibits the function of the target gene. The antisense RNA approach to gene suppression involves production of RNA sequences complementary to mRNA of the target gene (1); antisense RNA sequences are utilized either alone or in combination with other sequences that promote the cleavage of the target RNA (ribozymes) (2). Another approach involves the use of protein mutants that interfere with the function of the wild-type protein in a dominant fashion (3). In some cases, expression of the target gene or virus can be inhibited by overexpression of natural regulatory products, such as the TAR RNA of HIV (4).

Despite the ease of expressing antisense RNA for any cloned gene, many antisense RNA constructs have little or no biological effect (5–8). Some of the more effective antisense RNAs comprise only a portion of cDNA targeted for suppression. This portion in some but not all cases corresponds to the 5′ end of the target gene; there are no clear rules to predict which part of the cDNA would make the most effective antisense inhibitor (8–10). Dominant negative mutants may be derived from normal proteins by truncation of domains involved in specific functional interactions (3). Unless the domain structure of the target protein is well understood, however, one cannot predict which if any segments of the protein would act as dominant negative mutants. Thus, biologically active dominant negative mutants and antisense RNA constructs are mostly designed by inefficient trial-and-error approaches.

We have hypothesized that GSEs, encoding dominant negative mutant proteins or inhibitory antisense RNA sequences, can be generated by random DNA fragmentation and identified by functional selection for the phenotype associated with suppression of the target. To test this hypothesis, we have analyzed the ability of randomly fragmented bacteriophage lambda DNA to protect *E. coli* cells from lambda-induced lysis. By this approach, multiple GSEs encoding either protein or antisense RNA fragments have been isolated. Sequence analysis revealed strong sequence selectivity for both peptide- and antisense RNA-expressing GSEs. Analysis of the biological effects of individual GSEs indicated some previously unknown functions of lambda, including suppression of the cellular lambda receptor by a previously uncharacterized gene of the phage.

MATERIALS AND METHODS

Library construction and GSE selection

Lambda (CI857 ind1 Sam7) DNA was partially digested with DNAseI in the presence of Mn^{++}, to maximize the generation of blunt ends (11). After filling in the termini with T4 DNA polymerase and Klenow fragment of DNA polymerase I, the fragments were ligated with NcoI linkers. After NcoI digestion, 300–500 bp fragments were selected by agarose gel electrophoresis. The fragments were ligated with

* To whom correspondence should be addressed

dephosphorylated pKK233-2 vector (12), that had been modified by the insertion of the oligonucleotide CATGGTGACTGACTG-AAGCT into the NcoI and HindIII restriction sites, to provide for translation termination of inserts in all three open reading frames. A library of approximately 80,000 recombinant plasmids was generated in *E. coli* strain K12 PLK-F′ and amplified by growth on agar plates prior to selection for lambda resistance.

For lambda infection, cells carrying either the library or the control pKK233-2 vector were grown in LB with 0.5% maltose in the presence of 50 μg/ml ampicillin to OD_{600} = 0.3−0.5. Expression of the *trc* promoter of pKK233-2 was induced with 1 mM IPTG for 1−1.5 hours. (IPTG induction was subsequently found to have only a marginal effect due to high basal levels of expression from *trc* promoter, and it was omitted in later assays). Aliquots of 10^6 cells were resuspended in 100 μl of 10 mM $MgSO_4$ and mixed with 10^6 pfu of lambda (low m.o.i.) or 10^9 pfu (high m.o.i.). After 20 minutes incubation at 37°C, cells were plated on L agar plates with ampicillin and grown overnight.

In the initial experiment, lambda-resistant clones were selected by infection at low m.o.i., to account for the possibility that the anticipated GSEs would be unable to protect cells from simultaneous infection with multiple phage particles. At low m.o.i., 1%-3% of both library-derived and control bacteria survived the infection. Selection at low m.o.i. was followed by plasmid extraction from the surviving cells, re-transformation and a second round of phage infection, carried out at either high or low m.o.i. At this stage, 10% of the library cells (corresponding to 0.3% of the starting clones) survived the infection at both high and low m.o.i., in contrast to only 0.02% (at high m.o.i.) or 3% (at low m.o.i.) of the control bacteria. In a subsequent experiment, lambda-resistant clones were isolated from the random fragment library by a single round of selection at high m.o.i., and by this procedure 0.13% of the clones were found to be resistant to the phage. Clones isolated after single-step or two-step selection at high m.o.i. were used for further studies.

GSE characterization

Individual phage-selected plasmids were transformed into *E. coli* K12 LE392 or DH5α. Plasmid preparations were tested for the absence of lambda *dv* plasmids (13) by PCR amplification of sequences adjacent to the origin of lambda DNA replication, using the following primers: GGAGCGTAATGTGGCAGA (sense) and GCCTGCCTGTTGCTTGTT (antisense). Lambda *dv* contaminant was detected in some of the plasmid DNA preparations, most of which lost their ability to confer phage resistance after re-transformation and amplification in uninfected bacteria. Sequencing was carried out by a standard dideoxy technique.

Modified versions of GSEs of the *Ea8.5*, *V* and *oop/ori* classes were prepared by PCR synthesis using either lambda DNA or the corresponding plasmids as templates. The coding sequence of *Ea8.5* was synthesized using PCR primers GGAT-CCATGGGTATCAATGAGTGA (sense) and GGATCTGC-AGTTAATCATCTATATGT (antisense); the resulting PCR product encodes the Ea8.5 protein with a *ser→gly* substitution in the second codon. The version with a frameshift in the second codon was constructed using the same antisense primer and GG-ATCCATGGATGAGTATCAATGAGTTA as the sense primer. Other modified GSEs were synthesized and subcloned using the primers corresponding to the desired sequences and restriction sites.

Assays for GSE activity were carried out in *E. coli* strains K12 PLK-F′, LE392, NM-522 or DH5α. Lysogen induction was performed on *E. coli* K12 C600 (lambda cI857 N7 N53 S7) transformed with different GSEs. The prophage was induced by temperature shift to 42°C for 20 minutes followed by 1.5 hour at 37°C, and its titer was determined on *E. coli* LE392.

Analysis of *lamB* expression

Maltose utilization by bacteria transformed with *Ea8.5*-containing GSEs was analyzed by the color of colonies plated on McConkey media with 1% maltose and 50 μg/ml ampicillin. Bacterial RNA from cells transformed with *Ea8.5* GSEs was isolated using a nucleic acid extractor (Applied Biosystems, Model 340A) under the conditions recommended by the manufacturer. The RNA concentration was measured by the orcinol reaction (14). *malK-lamB* RNA expression was analyzed by northern hybridization using a PCR-amplified segment of the *lamB* gene (positions 4514−5005) (15) as a probe. Even loading of RNA was confirmed by ethidium bromide staining after electrophoresis.

RESULTS

Isolation of lambda-derived GSEs

Lambda DNA was fragmented by partial digestion with DNaseI, and NcoI linkers carrying the ATG translation initiation codon were added to the termini of the resulting fragments. Fragments of 300−500 bp size were isolated after NcoI digestion. These size limits were selected from the following considerations: (a) 100-150 amino acids is believed to be the size of most protein structural domains (16), (b) nucleic acids >300 bp show the highest hybridization efficiency and therefore are likely to be the most efficient antisense GSEs, and (c) the resulting fragments would not include the full-length CI repressor gene (713 bp) likely to provide an efficient but not novel GSE. The fragment mixture was inserted into a multicopy plasmid expression vector pKK233-2 (12), modified to provide for termination of translation of the inserted fragments in all three open reading frames.

The ligated mixture was used to transform a lambda-sensitive strain of *E.coli*, and a library of approximately 80,000 clones was obtained. Clones resistant to lambda-mediated lysis were selected from this library by either one or two rounds of phage infection, as described in Materials and Methods. Plasmids from individual phage-selected clones were then tested for the ability to render *E.coli* resistant to lambda upon re-transformation, and >90% of the plasmids were found to confer resistance to both the wild-type and CI^- strains of lambda. This property was maintained upon several rounds of plasmid propagation in uninfected bacteria. No plasmids conferring lambda resistance could be isolated from control bacteria transformed with insert-free vector. Thus, the random fragment selection strategy has resulted in the isolation of *bona fide* GSEs from lambda DNA.

51 of the isolated GSE clones were characterized by DNA sequencing. Eight clones were found in two or more identical copies; these may represent either siblings or, more likely, independently derived identical clones whose sequences reflect the constraints of functional selection or preferential DNaseI digestion. The sequenced GSEs were derived from eleven different regions of the phage genome. Eight classes of GSE contained fragments of lambda genes inserted in the sense orientation relative to the promoter. These inserts encoded either partial or complete open reading frames of specific phage proteins, starting either from the native translation initiation

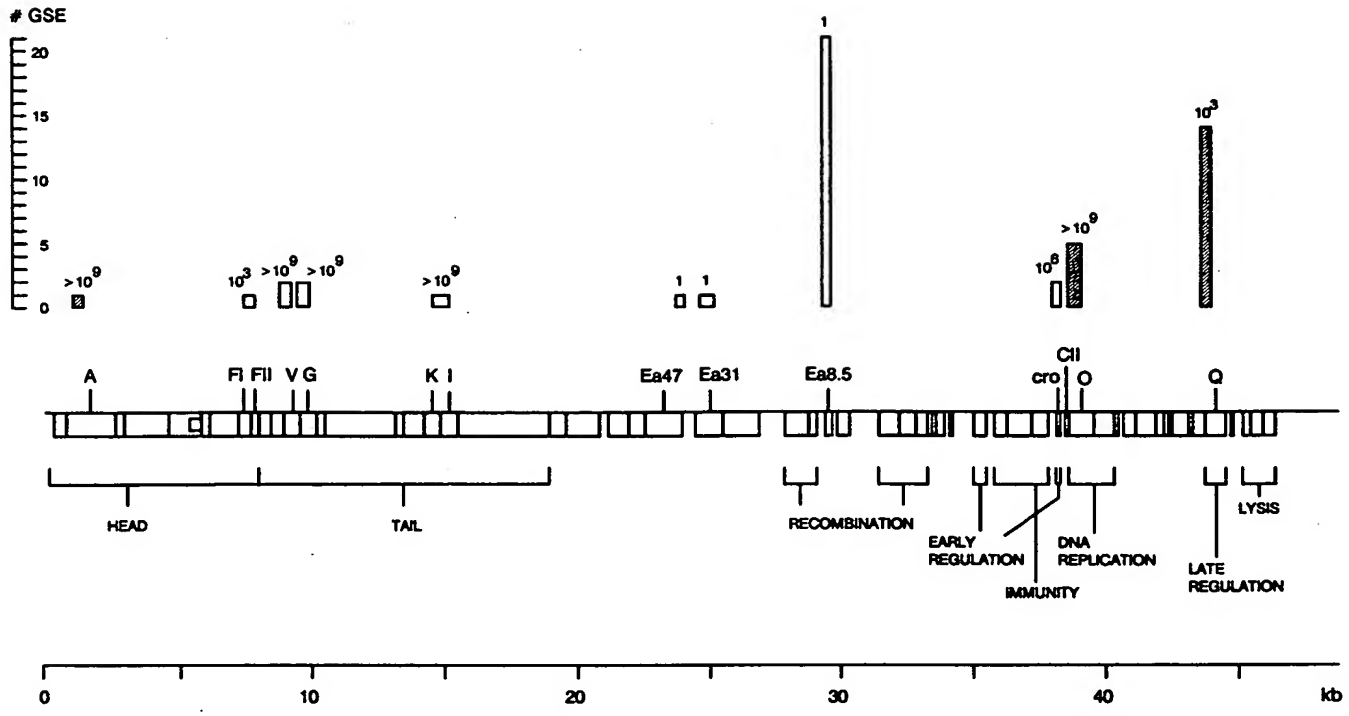

Figure 1. Distribution of GSEs in the lambda genome. Only the genes whose sequences were found in GSEs are indicated in the genetic map of lambda (30). Open bars: sense-oriented GSE. Hatched bars: antisense-oriented GSE. The height of the bars corresponds to the number of sequenced GSE clones for each class. The numbers on top of the bars indicate the extent of suppression of prophage induction by a representative clone of each class (the ratio of the phage titer obtained after induction of a control strain to the titer obtained from GSE-transformed clones).

codons of the corresponding genes, or from the linker-derived ATG codon joined in frame with the coding sequence, or (in one case) from an internal ATG codon located proximally to the linker. Three other classes contained lambda gene sequences inserted in antisense orientation relative to the promoter. The distribution of different classes of lambda-derived GSE is shown in Fig. 1.

The suppression efficiency of different classes of GSE was evaluated by the following tests. (a) Plating efficiency of transformed bacteria was measured after lambda infection at high m.o.i. Bacteria transformed with any of the GSE showed either none or a minor (<2-fold) decrease in the plating efficiency, in contrast to 0.02% of control bacteria surviving under the same conditions. All the GSE-transformed bacteria were equally resistant to CI^+ and CI^- strains of lambda, indicating that none of the GSEs exerted its effect by promoting lysogeny. (b) The decrease in phage titer was determined by plaque assay using the amounts of phage that produced 10^9 plaques in control bacteria. No plaques were discernible with most types of GSE, though some GSEs allowed for the formation of phage plaques at the incidence of 10^{-5} to 10^{-7}. These plaques reflected the appearance of GSE-insensitive mutant phage, since phage isolated from such plaques showed normal plating efficiency on the corresponding GSE transformants. (c) To determine the effect of GSEs on prophage induction, representative clones of each class were introduced into a strain of *E. coli* lysogenic for lambda, and the phage titer was determined after heat induction of the prophage. As indicated in Fig. 1, eight classes of GSE decreased the titer of the induced phage by three or more orders of magnitude, but GSEs of the other three classes had no effect on prophage induction.

Sense-oriented GSEs

The most abundant class of GSE carried sequences of the phage gene *Ea8.5*, inserted in the sense orientation. *Ea8.5* sequences were found in 21 (14 non-identical) of 51 sequenced GSEs. By colony hybridization, *Ea8.5* sequences were present in 40%-50% of all clones selected by either one or two rounds of phage infection. The *Ea8.5* gene, transcribed in the delayed early stage of lytic infection, is unnecessary for either lytic or lysogenic infection and encodes a 8.5 kD (93 amino acid) protein without a known function (17). Some of the GSE clones contained the entire *Ea8.5* gene (in the sense orientation), and other clones encoded truncated Ea8.5 proteins, missing 7 to 38 amino acids at the C-terminus or 3 to 10 amino acids at the N-terminus. The coding sequence of *Ea8.5*, free of flanking sequences, was synthesized by PCR and inserted into the pKK233-2 vector; the resulting clone protected *E. coli* from lysis by lambda. Introduction of a frameshift mutation into the second codon of *Ea8.5* abolished the GSE activity, thus indicating that this activity required expression of the Ea8.5 protein.

Ea8.5 expression in a lysogenic strain failed to suppress prophage induction, indicating that *Ea8.5* acted at the initial stages of phage infection, such as phage entry into the host cell, determined by the interaction of the phage with its cellular receptor. To test a role for the lambda receptor in *Ea8.5*-mediated resistance, we have infected *Ea8.5*-transformed cells with a recombinant phage $h^{80}imm\ \lambda$. This recombinant contains host-

range determinants of the phage ϕ80 (which enters the cell through a different receptor) replacing the corresponding portion of lambda DNA (18; N.C. Franklin, personal communication). The *Ea8.5* transfectants were sensitive to $h^{80}imm$ λ, suggesting that a change in the lambda receptor was responsible for the GSE activity of *Ea8.5*.

The cellular receptor recognized by lambda is the LamB protein that normally functions in the uptake of maltose (19); the *lamB* (or *malB*) gene is a part of *malK-lamB*, one of the three maltose operons of *E. coli* (15). We have found that bacteria expressing *Ea8.5* were deficient in maltose metabolism, judging by the white color of colonies grown on McConkey media with maltose (wild-type colonies appear red on this media). This effect was specific to maltose, and was not observed with galactose, lactose, mannose or arabinose. A deficiency in LamB alone would have been insufficient to produce white colonies on McConkey media with maltose (20 and our data not shown). We have hypothesized therefore that *Ea8.5* expression affected the entire maltose operon(s), most probably at the level of transcription. Northern hybridization with a *lamB* probe (Fig. 2) showed the disappearance of detectable *malK-lamB* RNA in cells transformed with full-length *Ea8.5* but not with its frameshift variant; these results were reproduced in two other bacterial strains (data not shown). Thus *Ea8.5* expression leads to the inhibition of the maltose operon encoding the lambda receptor.

Most of the isolated *Ea8.5* GSEs expressed truncated rather than full-length versions of the Ea8.5 protein. As shown in Table 1, increasing truncation of the protein at the N- or C-terminus was associated with a gradual change in the color of the colonies on McConkey media with maltose from white to pink to red; further truncation at the C-terminus, however, again rendered the colonies white. Transformation of three different strains of *E. coli* with truncated *Ea8.5* clones giving rise to pink or red colonies on McConkey media with maltose resulted in strongly decreased but detectable expression of *malK-lamB* RNA (Fig. 2 and data not shown), indicating that the phage receptor was only partially suppressed in the transformed clones.

The composition of the sense-oriented GSEs distinct from *Ea8.5* is shown in Table 2. Two classes of GSE, each represented by a single sequenced clone, contained portions of genes with unknown functions. These genes, *Ea31* and *Ea47*, belong to the same P_L operon that includes *Ea8.5* (17). Both GSEs were inserted in the sense orientation and encoded C-terminal segments of the corresponding proteins. Like *Ea8.5*, these GSEs failed to suppress lysogen induction and did not confer resistance to $h^{80}imm$ λ, suggesting that they could also act at the level of the phage entry. These clones, however, did not change the red color of colonies on McConkey media with maltose, indicating that they had no major effect on the maltose operon.

Another class of GSE, represented by two sequenced clones, contained the entire gene *cro* in the sense orientation. This gene encodes a regulatory protein known to suppress the expression of the early genes of lambda (21), and therefore its GSE effect was anticipated.

Four classes of GSE encoded truncated forms of structural proteins of the phage particle. One clone spanned the *FI* and *FII* genes of the phage head, encoding a C-terminal portion of the first and the N-terminal portion of the second protein. Another GSE encoded portions of two tail proteins, K and I. Interestingly, each of the two other classes of GSE, encoding C-truncated forms of tail proteins V or G, included two independent clones that encoded exactly the same segments of the corresponding proteins (Table 2), truncated at the C-terminus. In one case (G), the two GSEs differed at their 5′ ends but coincided at the 3′ ends. *V*-derived GSEs had different 5′ ends but terminated at different bases within the same codon at the 3′ end. The coincidence of the protein segments encoded by these non-identical GSE clones can be most redily explained by strong functional selection at the protein level. Protein-mediated action of the GSEs derived from the *V* gene was verified by preparing clones with PCR-synthesized inserts, encoding either the first 145 codons of *V*,

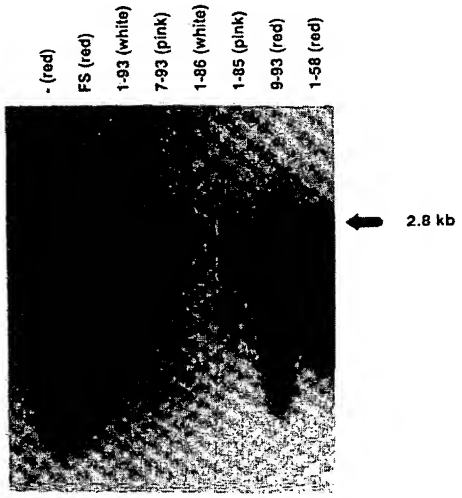

Figure 2. Effect of *Ea8.5* clones on *malK-lamB* RNA expression. Each lane contains 15 μg of total RNA from *E. coli* K12 LE392 transformed either with the insert-free plasmid vector (−) or with plasmids carrying *Ea8.5* sequences. The amino acids of the Ea8.5 protein encoded by the plasmids (1−93, full length; FS, frameshift) and the color of the corresponding colonies on McConkey media with maltose are indicated.

Table 1. Compositions and phenotypes of *Ea8.5*-derived GSEs

Position[a]	Amino acid residues of Ea8.5	Color on McConkey media with maltose
Full-length:		
29762−29269	1−93	White
29749−29353	1−93	White
29718−29243	1−93	White
29703−29300	1−93	White
N-truncated:		
29646−29084	4−93	White
29638−29217	7−93	Pink
29637−29155	7−93	Pink
29632−29242	9−93	Red
29626−29206	11−93	Red
C-truncated:		
29793−29398	1−86	White
29768−29398	1−86	White
29793−29400	1−85	Pink
29850−29480	1−58	Red
29931−29489	1−55	White
PCR-synthesized:		
29655−29374	1−93	White
Same, frameshift	−	Red

[a]Numbered according to ref. 30.

as found in the GSEs, or a variant of the same sequence with a nonsense mutation in the fourth codon. The clone encoding truncated V protected *E. coli* from lambda, but the nonsense mutation abolished its GSE activity.

Antisense-oriented GSEs

Among the GSEs encoding antisense RNA, one sequenced clone (positions 1050–1470) contained an internal segment of gene *A*, involved in DNA packaging. Two other classes of antisense GSE were represented by multiple clones. One of these classes included 12 non-identical clones (14 total) encoding RNA complementary to the 5′ portion of the gene *Q*, a positive regulator of late transcription (22). All the GSEs in this class (Fig. 3A) overlapped with a naturally occurring antisense transcript P_{aQ} (approximately 220 bases long), that normally downregulates *Q* expression (1,23). In addition to the complete or partial P_{aQ} sequence, the GSEs contained variable lengths of flanking sequences extending downstream from P_{aQ}. In contrast to the flexible composition of downstream sequences, none of the GSEs initiated more than 70 bp upstream from the P_{aQ} promoter, with seven of twelve different GSEs initiating within 16 bp from each other. The absence of the upstream sequences in the P_{aQ}-containing GSEs indicates functional selection against sequences complementary to the 3′ end of *Q*.

A particularly interesting group of four different GSEs (five total) encoded almost identical antisense RNA sequences, corresponding to the 3′ end of the gene *CII* (regulator of lysogeny) and the 5′ half of gene *O* that codes for a protein involved in lambda DNA replication; the origin of replication, located in the middle of *O*, was also present in these clones (Fig. 3B). The *CII* portion of the GSEs included a naturally occurring antisense transcript termed *oop* (77 bases long), which normally serves to suppress *CII* (1,24). Overexpression of the *oop* sequence has been shown to enhance lytic infection (25), an effect opposite to that of our GSEs. To explain this paradox, we hypothesized that the *oop* portion of the GSEs, complementary to *CII*, serves to promote a strong complementary interaction between the sense and the antisense RNAs, but the actual suppression is determined by another portion of the same GSE, derived from the *O* gene. To test this hypothesis, we have generated two truncated variants of these *oop/ori* GSEs (Fig. 3B). One variant was missing a 93 bp segment including most of the *oop* sequence, but still contained the 5′ portion of gene *O* including the origin of replication. The second variant had a deletion of a 158 bp segment of *O* comprising the origin of replication but still contained the *oop* sequence and the 5′ end of *O*. Cells transformed with either of the truncated plasmids showed no detectable resistance to lambda, indicating that both of the deleted segments were crucial for the GSE activity of *oop/ori*.

Table 2. Sense-oriented GSEs (other than *Ea8.5*)

Position in lambda DNA[a]	Gene(s)[b]	GSE peptide[c]
7317–7732	FI (117), FII (117)	38–117, 1–40
8800–9390	V (256)	1–145
8848–9391	V (256)	1–145
9650–10052	G (140)	1–113
9660–10052	G (140)	1–113
14397–15138	K (198), I (223)	40–198, 1–121
22997–22688[d]	Ea47 (410)	323–410
25224–24302[d]	Ea31 (296)	81–296
37939–38359	cro (66)	1–66
38029–38389	cro (66)	1–66

[a]Numbered according to ref. 30.
[b]The total number of amino acid residues in the corresponding protein is shown in parentheses.
[c]Position of the peptide in the corresponding protein.
[d]Transcribed in the direction opposite to that of numbering.

DISCUSSION

We have tested a concept that genetic suppressor elements (GSEs), encoding dominant negative mutant proteins or inhibitory antisense RNA sequences, can be generated by random DNA fragmentation and identified by expression selection. Using inhibition of lytic infection by bacteriophage lambda as a model system, we have found that DNaseI fragmentation of lambda DNA, followed by functional selection of fragments that render E. coli resistant to the virus, leads to the isolation of biologically active GSEs that inhibit viral infection by interfering with the functions of different viral or cellular genes. GSE derivation by our procedure requires no prior knowledge of the RNA or protein structure, or even the nature of the gene(s) to be suppressed.

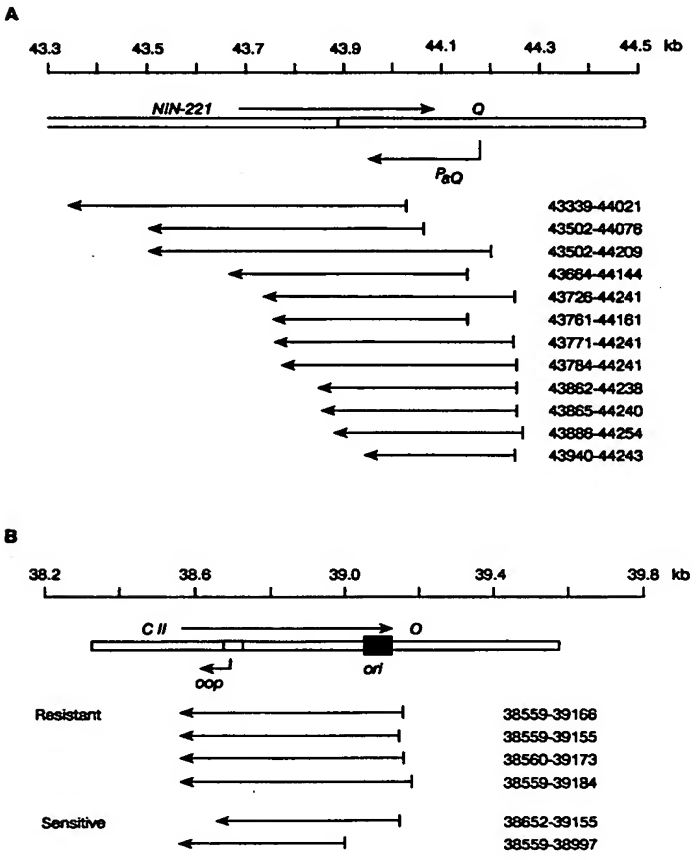

Figure 3. A. Distribution of the P_{aQ}-related GSEs. Arrows indicate the direction of transcription. Map position of the antisense P_{aQ} transcript is according to (23). B. Distribution of the *oop/ori* class of GSEs and the corresponding lambda resistance phenotypes. Arrows indicate the direction of transcription. Map position of the antisense *oop* transcript is according to (24). The four top clones were obtained by GSE selection. The two bottom clones were constructed by PCR synthesis using the corresponding primers.

The isolated lambda GSEs were derived from eleven different regions of the phage genome. Sequence analysis indicated that most classes of GSE acted by inhibiting the function of the corresponding genes of lambda, but at least one and possibly three classes exerted their effect by inhibiting the host gene(s) required for lambda infection. The latter GSE classes corresponded to early lambda genes with previously unknown functions. Our results suggest a biological role for these 'accessory' genes of lambda (17), that are unnecessary for either lytic or lysogenic infection. Specifically, we have demonstrated that the *Ea8.5* gene prevented phage infection by blocking the synthesis of the LamB phage receptor at the RNA level. Truncated forms of two other 'accessory' genes, *Ea31* and *Ea47*, are also likely to interfere with the phage entry, since these GSEs prevented infection with lambda but not with a recombinant phage carrying the host range determinant of ϕ80, and they failed to inhibit induction of the lambda lysogen. *Ea31* and *Ea47* sequences, however, did not inhibit maltose metabolism, indicating that these GSEs blocked the infection by a mechanism different from that of *Ea8.5*.

Suppression of the expression, processing or availability of the cellular receptor is a known evolutionary mechanism developed by different groups of viruses for preventing superinfection with a second virus (26,27), but this function has not been previously associated with the lytic cycle of lambda. It seems reasonable to suggest that the normal function of *Ea8.5* and other genes capable of inhibiting lambda infection is to prevent superinfection at an early stage of the lytic cycle. Inhibition of LamB synthesis at the RNA level by *Ea8.5* may be supplemented by the function of *Ea31*, *Ea47*, and possibly some other 'accessory' genes, whose products may interfere directly with either LamB or some other cellular proteins involved in phage adsorption or penetration.

Several other results of GSE analysis raise new questions concerning the biology of lambda infection. One unexpected observation was the effect of the GSEs derived from the structural genes of lambda, that should selectively interfere with the assembly of viral particles at the late stage of the infection. Nevertheless, these GSEs not only blocked the production of viral progeny but also prevented cell killing after phage infection at high m.o.i. Another paradoxical finding was the prevention of lysis by antisense GSEs containing a 'native' antisense RNA sequence, *oop*, that normally serves to enhance rather than suppress the lytic infection. This *oop/ori* class of antisense RNA, represented by several nearly identical clones, required both a segment corresponding to the origin of lambda DNA replication, and the *oop* sequence for its suppressive action. The strong sequence specificity and the very high efficiency of suppression by this class of GSE raise a question whether *oop/ori* antisense RNA may exist in nature as a presently unknown regulatory product of lambda. The specific function of the *ori* portion of these GSEs and its conceivable effect on DNA replication also represent an interesting issue for future studies.

A general question in the area of targeted gene suppression is whether antisense RNAs or dominant negative mutants constitute more efficient inhibitors. In the present study, we addressed this question in the lambda system by generating a representative GSE library, where both types of elements were placed into the same vector and selected for biological activity under the same conditions. In the starting library, antisense RNA-expressing clones for any given gene were more abundant than clones expressing truncated proteins with potential dominant negative activity, since most of the sense-oriented clones inserted out of frame with the ATG codon of the linker would not give rise to truncated normal proteins. Nevertheless, biologically active GSEs derived from the essential lambda genes encoded in most cases truncated proteins rather than antisense RNA. In fact, aside from the GSEs that incorporated evolutionarily selected 'native' antisense sequences, there was only one antisense GSE in the entire set. The observed limited efficiency of suppression by antisense constructs is in agreement with previous observations on phage lambda (7) and other organisms (5,6), and it underscores the importance of dominant negative mutant proteins as efficient tools for gene suppression (3).

The concept of using truncated proteins as dominant negative mutants (3) is based on the idea that proteins possessing domains involved in interactions with different molecules may form defective multimolecular aggregates if one of their domains is deleted or altered. In our analysis of sense-oriented GSEs, we have asked how precise should be the deletion that gives rise to a dominant negative mutant. For two structural genes of the phage (*V* and *G*), we have found two independent GSE clones encoding truncated forms of each of the corresponding proteins. Surprisingly, in both cases the truncated portions of the proteins coincided to a single amino acid between the two GSEs. This result indicates extremely strong structural limitations of truncated proteins that act as dominant negative mutants and shows that our use of a non-specific procedure for DNA fragmentation was essential for the isolation of this type of GSEs. Thus, selection of random fragments with biological activity provides a new approach to the delineation of functional protein domains.

Strong sequence selectivity was also associated with the two major classes of antisense RNA-expressing GSE. In particular, examination of the P_{aQ}-containing antisense GSEs indicates exclusion of sequences complementary to the 3′ portion of *Q* RNA and located more than 70 bp upstream from the P_{aQ} promoter. The apparent negative effect of specific RNA sequences on antisense inhibition may explain the failure of some full-length antisense constructs to inhibit the expression of corresponding genes. In contrast, the example of the *oop/ori* class of GSEs shows cooperative interaction of two antisense RNA elements, derived from different cistrons of a polycistronic message.

Identification of antisense RNA sequences capable of suppressing a target gene is a major goal in designing antisense RNA vectors for gene therapy and oligonucleotides that would have the desired suppressive effect in a chemically synthesized form. There are as yet no reliable procedures for predicting which antisense RNA sequences would be active in biological assays. The results of our study indicate that random fragment selection provides such a procedure. In this regard, it would be important to determine the minimum length of antisense GSEs that can be isolated by random fragment selection.

Our work with bacteriophage lambda may serve as a prototype for similar studies aimed at the derivation of GSEs providing the resistance to various pathogens (28). Furthermore, the same strategy is applicable to many other selectable phenotypes associated with decreased gene function. Such phenotypes may include, for example, changes in the expression of specific antigens, neoplastic transformation associated with inhibition of tumor suppressor genes, and resistance to drugs whose cytotoxic action is potentiated by a target enzyme. Thus, we have used the latter selection strategy to obtain a series of sense- and antisense-oriented GSEs suppressing the function of human topoisomerase II, a common target for many anti-cancer drugs (A.V. Gudkov, C. Zelnick, A. Kazarov, D.P. Suttle, W.T. Beck

and I.B.R., manuscript in preparation). We have also used random fragment libraries to suppress several other cellular and viral targets in mammalian cells (T.A.H., E.B. Mechetner, A.V. Gudkov and I.B.R., unpublished data).

The results of the present study show that the random fragment selection strategy not only allows one to derive efficient GSEs, but also leads to identification of novel genes associated with specific phenotypes. Expression selection of random DNA fragments, derived from total cDNA or genomic DNA, would provide a general approach to cloning of recessive genes. Antisense cDNA libraries (29) provide an alternative route to the same goal, but their efficiency is limited by the fact that not all the genes can be adequately inhibited by antisense RNA (8). Furthermore, random fragment selection allows one to identify not only the relevant genes, but also specific functional domains of the corresponding proteins.

ACKNOWLEDGEMENTS

We would like to thank N.C. Franklin for the gift of $h^{80}imm$ λ, J. W. Roberts for *E. coli* K12 C600 lysogen, T. Kolesnikova and D. Tarassiewicz for assistance with some experiments, and A. Dayn, A. Gudkov, S. Mirkin and W. Szybalski for helpful discussions. Supported by grants CA39365 and CA40333 from the National Cancer Institute and a Faculty Research Award from the American Cancer Society, Inc. (I.B.R.).

REFERENCES

1. Takayama, K.M. and Inouye, M. (1990). Crit. Rev. Biochem. Mol. Biol., **25**, 155–184.
2. Cameron, F.H. and Jennings, P.A. (1989). Proc. Natl. Acad. Sci. USA., **86**, 9139–9143.
3. Herskowitz, I. (1987). Nature, **329**, 219–222.
4. Sullenger, B.A., Gallardo, H.F., Ungers, G.E. and Gilboa, E. (1990). Cell **63**, 601–698.
5. Kerr, S.M., Stark, G.R. and Kerr, I.M. (1988). Eur. J. Biochem., **175**, 65–73.
6. Leiter, J.M., Krystal, M. and Palese, P. (1989). Virus Res., **14**, 141–159.
7. Hasan, N., Somasekhar, G. and Szybalski, W. (1988). Gene, **72**, 247–252.
8. Van der Krol, A.R., Mol, J.N. and Stuitje, A.R. (1988). Biotechniques, **6**, 958–976.
9. Daugherty, B.L., Hotta, K., Kumar, C., Ahn, Y.H., Zhu, J. and Pestka, S. (1989). Gene Anal. Tech., **6**, 1–16.
10. Rhodes, A. and James, W. J. (1990). J. Gen. Virol., **71**, 1965–1974.
11. Sambrook, J., Fritsch, E.F. and Maniatis, T. (1989). Molecular Cloning: A Laboratory Manual. Cold Spring Harbor Laboratory Press, Cold Spring Harbor.
12. Amann, E. and Brosius, J. (1985). Gene, **40**, 183–190.
13. Berg, D.E. (1971). In Hershey, A.D. (ed.), The Bacteriophage Lambda. Cold Spring Harbor Laboratory Press, Cold Spring Harbor, pp. 667–678.
14. Lin, R.I.-s. and Schjeide, O.A. (1969). Anal. Biochem., **27**, 473–483.
15. Debarbouille, M., Cossart, P. and Raibaud, O. (1982). Mol. Gen. Genet., **185**, 88–92.
16. Janin, J. and Wodak, S.J. (1983). Mol. Biol., **42**, 21–78.
17. Court, D. and Oppenheim, A. (1983). In Hendrix, R.W., Roberts, J.W., Stahl, F.W. and Weisberg, R.A. (eds.), Lambda II. Cold Spring Harbor Laboratory Press, Cold Spring Harbor, pp. 251–278.
18. Franklin, N.C. (1967). Genetics, **57**, 301–318.
19. Randall-Hazelbauer, L. and Schwartz, M. (1973). J. Bacteriol., **116**, 1436–1446.
20. Boulain, J.C., Charbit, A. and Hofnung, M. (1986). Mol. Gen. Genet., **205**, 339–348.
21. Gussin, G., Johnson, A., Pabo, C. and Sauer, R. (1983). In Hendrix, R.W., Roberts, J.W., Stahl, F.W. and Weisberg, R.A. (eds.), Lambda II. Cold Spring Harbor Laboratory Press, Cold Spring Harbor, pp. 93–122.
22. Friedman, D. and Gottesman, M. (1983). In Hendrix, R.W., Roberts, J.W., Stahl, F.W. and Weisberg, R.A. (eds.), Lambda II. Cold Spring Harbor Laboratory Press, Cold Spring Harbor, pp. 21–52.
23. Hoopes, B.C. and McClure, W.R. (1985). Proc. Natl. Acad. Sci. USA, **82**, 3134–3138.
24. Krinke, L. and Wulff, D.L. (1987). Genes Dev., **1**, 1005–1013.
25. Takayama, K.M., Houba-Herin, N and Inouye, M. (1987). Mol. Gen. Genet., **210**, 184–186.
26. Simon, K.O., Cardamone, J.J., Whitaker-Dowling, P.A., Youngner, J.S. and Widnell, C.C. (1990). Virology, **177**, 375–379.
27. Garcia, J.V. and Miller, A.D. (1991). Nature, **350**, 508–511.
28. Baltimore, D. (1988). Nature, **335**, 395–396.
29. Deiss, L.P. and Kimchi, A. (1991). Science, **252**, 117–120.
30. Daniels, D., Schroeder, J., Szybalski, W., Sanger, F. and Blattner, F. (1983). In Hendrix, R.W., Roberts, J.W., Stahl, F.W. and Weisberg, R.A. (eds.), Lambda II. Cold Spring Harbor Laboratory Press, Cold Spring Harbor, pp. 467–518.

MOLECULAR AND CELLULAR BIOLOGY, Mar. 1991, p. 1360–1371
0270-7306/91/031360-12$02.00/0

Vol. 11, No. 3

Episome-Generated N-*myc* Antisense RNA Restricts the Differentiation Potential of Primitive Neuroectodermal Cell Lines

LUKE WHITESELL,* ANGELO ROSOLEN, AND LEONARD M. NECKERS

Tumor Cell Biology Section, Clinical Pharmacology Branch, National Cancer Institute, Bethesda, Maryland 20892

Received 1 June 1990/Accepted 30 November 1990

Neuroectodermal tumors of childhood provide a unique opportunity to examine the role of genes potentially regulating neuronal growth and differentiation because many cell lines derived from these tumors are composed of at least two distinct morphologic cell types. These types display variant phenotypic characteristics and spontaneously interconvert, or transdifferentiate, in vitro. The factors that regulate transdifferentiation are unknown. Application of antisense approaches to the transdifferentiation process has allowed us to explore the precise role that N-*myc* may play in regulating developing systems. We now report construction of an episomally replicating expression vector designed to generate RNA antisense to part of the human N-*myc* gene. Such a vector is able to specifically inhibit N-*myc* expression in cell lines carrying both normal and amplified N-*myc* alleles. Inhibition of N-*myc* expression blocks transdifferentiation in these lines, with accumulation of cells of an intermediate phenotype. A concomitant decrease in growth rate but not loss of tumorigenicity was observed in the N-*myc* nonamplified cell line CHP-100. Vector-generated antisense RNA should allow identification of genes specifically regulated by the proto-oncogene N-*myc*.

myc family proto-oncogenes have long been hypothesized as regulators of gene expression because of their demonstrated nuclear localization and their conversation of motifs previously identified in transcription factors, i.e., leucine zipper and helix-loop-helix domains (5, 18). Nonetheless, the genes that they regulate are not known. Unlike the fairly ubiquitous expression of c-*myc* in proliferating tissues of the adult organism, high-level expression of N-*myc* has been shown to be temporally and spatially restricted during embryogenesis, with a dramatic decline noted upon adult maturation (17, 32). Differential expression has been suggested to be involved in the regulation of organ-specific growth and differentiation of such diverse cell types as brain, kidney, and B lymphocytes. Perhaps not surprisingly then, N-*myc* amplification and aberrant expression have been noted in a variety of neuroectoderm-derived cancers (12, 13, 19, 26).

Certain primitive or embryonal tumors of childhood provide a unique opportunity to examine the precise role that N-*myc* may play in regulating developing systems. Many established, N-*myc*-amplified neuroblastoma cell lines have been reported to be composed of at least two distinct morphologic cell types that display variant phenotypic characteristics and spontaneously interconvert, or transdifferentiate (4, 20, 24). The predominant cell type, termed N, is neuroblastic and has a small, refractile cell body, long neuritic processes, dense core vesicles, and neurotransmitter biosynthetic enzymes. This cell type is independently tumorigenic in that pure N-type subclones are able to grow in soft agar and in nude mice. The other type, termed S, is flat, shows abundant cytoplasm, and is substrate adherent. It does not extend processes and shows no transmitter synthesis, but it does express tyrosinase, vimentin, and fibronectin. Subclones of this type are reported not to clone in soft agar nor form tumors in nude mice. Although not extensively characterized, N-*myc* expression in an amplified line has been reported to be limited largely to the neuroblastic variant in short-term culture (16).

The mechanisms that regulate S and N interconversion are completely unknown. Because differential expression of the N-*myc* gene had been described in N- and S-type neuroblastoma cells, we reasoned N-*myc* might play a regulatory role in the transdifferentiation process. Previously we showed that exogenous addition of a small N-*myc* antisense oligonucleotide was capable of decreasing N-*myc* expression in short-term culture of the N-*myc*-nonamplified neuroepithelioma cell line CHP-100, while a sense oligonucleotide had no effect (22). Observation of these antisense oligonucleotide-treated cultures demonstrated concomitant effects on growth and apparent cellular heterogeneity. To characterize the effects of N-*myc* inhibition on the transdifferentiation process, more sustained inhibition of N-*myc* expression in many more cells than can be achieved with exogenous addition of oligonucleotides is necessary. Stable transfection of cultured cells with antisense RNA-expressing vectors allows continuous generation of antisense sequences within the cell itself (9). Previous attempts to use such vectors have been limited by the need to generate antisense sequences in many-fold excess of the target sequence in order to effectively suppress expression. Even with the strongest eukaryotic promoters, conventional integrating vectors are not able to suppress expression of an amplified gene such as N-*myc* in neuroblastoma. Episomal replicons have been developed as a means of amplifying vector copy number in cells and circumventing the positional effects on transcription associated with chromosomal integration (14). The Epstein-Barr virus origin of replication and nuclear antigen I have been shown to confer episomal replication capacity to plasmid vectors in a range of human cell types (31). In addition, upon removal of selective antibiotic pressure, episomal replicons are readily lost from culture by dilution and their potential antisense effects are reversed (8).

To study the role that N-*myc* might play in regulating transdifferentiation, we have developed a vector-generated antisense approach to produce metastable somatic mutants of human cell lines carrying both normal and amplified

* Corresponding author.

N-*myc* sequences. Unlike the homologous recombination strategy recently reported (3), our N-*myc* antisense approach is able to suppress expression reversibly and in cells carrying many copies of the target gene. We report the effects of such suppression on the transdifferentiation process and the consequences observed for growth rate and tumorigenicity in nude mice.

MATERIALS AND METHODS

Construction of vectors. The episomally replicating vector pREP3 was obtained as a generous gift from M. Tykocinski and has been described elsewhere in detail (7). A previously described 1-kb DNA fragment, pNb1, which begins in the first intron and extends downstream through the translation initiation site of the human N-*myc* gene, was obtained as an *Eco*RI-*Bam*HI insert from Lofstrand Labs, Gaithersburg, Md. (26). After fill-in with the Klenow fragment of DNA polymerase I (Bethesda Research Laboratories), the fragment was ligated bluntly into the phosphatase-treated (Boehringer) *Pvu*II site of the pREP3 polylinker, using T4 DNA ligase (New England BioLabs). Ampicillin-resistant colonies were screened by using a colony lift procedure with ^{32}P-pNb1 as the probe (Colony/Plaque Screen; NEN). Presence of the insert was confirmed by Southern blot of minipreps made from positive colonies. Preps were subjected to restriction analysis to determine the orientation of pNb1 insertion by using an asymmetric *Sst*I site, and plasmid was then prepared from sense, antisense, and unmodified vector clones by using standard alkaline lysis-cesium chloride centrifugation procedures (Fig. 1).

Electroporation and selection of cells. The peripheral neuroepithelioma cell line CHP-100 and the neuroblastoma cell line IMR-32 have been well characterized (25, 29). They were maintained as monolayer cultures in complete medium consisting of RPMI 1640 with 10% heat-inactivated fetal bovine serum, 15 mM *N*-hydroxyethylpiperazine-*N'*-2-ethanesulfonic acid (HEPES), 100 U of penicillin G per ml, 100 μg of streptomycin per ml, and 2 mM L-glutamine (all from GIBCO Laboratories). Cells were passaged at a 1:10 ratio when confluent (approximately 7 to 10 days) by trypsinization for 5 min at 37°C. Distinct biphenotypic morphologies were consistently maintained in both cell lines as previously reported (22, 25). Cells were confirmed negative for mycoplasma by standard techniques. In addition, cell line CHP-100 was karyotyped by an independent laboratory (H&W Cytogenetic Services, Inc., Lovettsville, Va.). Marked aneuploidy was noted with chromosome number ranging from 60 to 85, with no cytogenetic evidence of distinct cell populations. All experiments were performed on low-passage stock cultures kept frozen under liquid nitrogen vapor.

Single-cell clones were derived from wild-type CHP-100 by plating mixed-phenotype cultures at very low density and allowing isolated colonies to form. After 2 to 3 weeks, macroscopic colonies of grossly flat, round, or mixed morphology (as determined by phase-contrast microscopy) were readily apparent. Individual colonies were scraped from the dish and expanded for cryopreservation and further studies. Although what we describe as CHP-100 round clones resemble the previously described N-type cells of many neuroblastoma lines and flat clones resemble S-type cells, we have elected to use the terms round and flat in reference to the subclones of this biologically distinct neuroepithelioma cell line.

Electroporation was performed at 20°C on trypsin-harvested subconfluent cells, using 2×10^6 cells in 1 ml of Dulbecco modified Eagle medium (GIBCO) and a Bethesda Research Laboratories Cell-Porator; 15 μg of plasmid was used per transfection. Field strength was 875 V/cm; pulse length was 3.7 ms for CHP-100 and 13.2 ms for IMR-32. Ten minutes after electroporation, cells were resuspended in complete medium and plated in 100-mm tissue culture dishes. The selective antibiotic hygromycin B (Calbiochem) was added 48 h after electroporation at 50 μg/ml for CHP-100 and 200 μg/ml for IMR-32 (these concentrations had been previously shown to kill 100% of sham-transfected cells in 7 days). Widely separated resistant colonies were apparent 10 to 14 days postelectroporation; individual colonies were scraped from the plate at 21 days, examined for morphology, and expanded for further studies and cryopreservation.

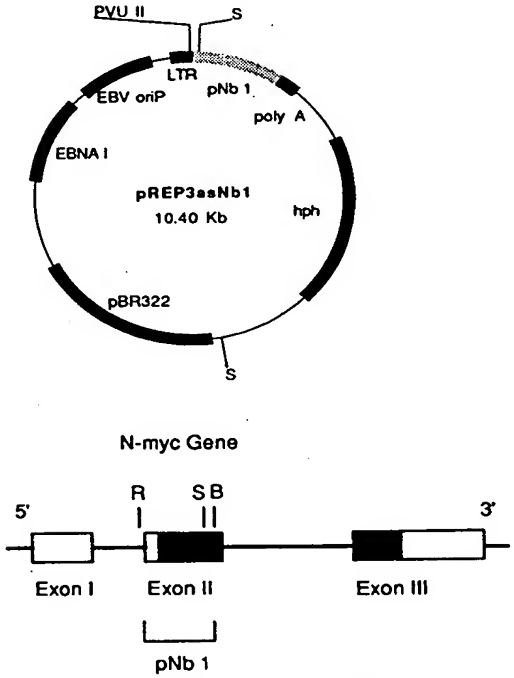

FIG. 1. Structure of the human N-*myc* gene and construction of a recombinant episomal replicon. Boxes in the diagram of N-*myc* represent exons, with coding sequences indicated by darkened portions. Darkened boxes in the map of the vector represent coding sequences. The stippled box represents the N-*myc* sequence cloned into the vector in the antisense orientation. A similar construct containing the identical N-*myc* fragment cloned in the sense orientation was made. R, *Eco*RI; B, *Bam*HI; S, *Sst*I. The map of the vector is not drawn to scale.

Immunocytochemical analysis of N-*myc* protein. Control and transfected cells were harvested by trypsinization, and cytopreps were prepared with 100,000 cells per slide, using a Shandon Cytospin 2 centrifuge. Slides were air dried and stained by a modification of the procedure reported by Ikegaki et al. (10). Briefly, slides were fixed in 3.7% fresh paraformaldehyde for 5 min and then permeabilized for 5 min in 2% Triton X-100. Slides were then blocked for 1 h at 37°C with a solution of 1.5% bovine serum albumin (BSA), 2.0% Carnation powdered milk, and 10% goat serum. The previously described N-*myc*-specific hybridoma supernatant NMC II-100 was applied undiluted as the primary antibody for 1 h at 20°C (10). Duplicate slides were incubated with the

irrelevant supernatant P3X63Ag8 (American Type Culture Collection [ATCC], Rockville, Md.) as a background control. After rinsing and reblocking, biotin-conjugated goat anti-mouse antibody (Kirkegaard and Perry Labs, Gaithersburg, Md.) was applied at 1:200 for 30 min. Avidin-biotin-peroxidase complex (Vectastain ABC kit; Vector Labs) was next applied as directed for 30 min. Finally, slides were developed with diaminobenzidene-nickel chloride-hydrogen peroxide according to the kit instructions, counterstained, and mounted. Cytopreps as well as chamber slides on which cells had been cultured (Lab-Tek, Nunc) were also stained with the Diff-Quik differential staining kit (Baxter, Scientific Products Division) for simple morphologic evaluation.

Western immunoblotting. Oncoprotein expression was evaluated by using a modification of the procedure of Ikegaki et al. (10). Cell extracts were made in 2× phosphate-buffered saline (PBS) containing 1% Nonidet P-40, 0.5% sodium deoxycholate, 0.1% sodium dodecyl sulfate (SDS), 1 mM EDTA, 10 μg of leupeptin per ml, 75 μg of phenylmethylsulfonyl fluoride per ml, and 1 mg of aprotinin per ml at 50×10^6 cells per ml. Extraction was performed on ice for 15 min with occasional vortexing. Lysates were spun in an Eppendorf microfuge at 4°C and maximum speed for 10 min. The supernatant was collected, and an aliquot was assayed for total protein concentration by using a Coomassie dye-based kit (Bio-Rad) and immunoglobulin G standard. Lysates were stored at −70°C until use. Standard SDS-polyacrylamide gel electrophoresis was performed through 7.5% resolving gels under reducing conditions, using a Hoefer minigel apparatus and 60 μg of total protein per lane. Proteins were transferred to nitrocellulose by using a Multiphor II electrophoresis unit (LKB) as instructed by the manufacturer. After transfer, nitrocellulose was blocked with the milk-containing solution described above for 30 min at 37°C. Blots were then incubated overnight at 4°C with rocking in 5 ml of undiluted culture supernatant. The N-*myc*-specific monoclonal antibody NMC II-100 (see above) and the c-*myc*-specific monoclonal antibody MYC CT14-G4.3 (ATCC, Rockville, Md.) were used as primary antibodies. No antibody cross-reactivity was noted under the conditions described. After primary incubation, blots were rinsed, fixed in cold 0.25% glutaraldehyde, reblocked with 0.1% BSA in PBS, and incubated with biotinylated goat anti-mouse immunoglobulin (1:200) for 2 h at 20°C. After rinsing, avidin-biotin-peroxidase complex was applied (see above) for 1.5 h. Blots were again rinsed and finally developed in 4-chloro-1-naphthol for 30 to 60 min at 20°C.

Immunophenotypic analysis of CHP-100 differentiation. Expression of specific cell surface markers was evaluated by indirect immunofluorescence using three well-characterized murine monoclonal antibodies. Anti-Leu 7 (CD 57; Becton Dickinson) recognizes a carbohydrate epitope present on the human N-CAM molecule. HFN 7.1 (CRL 1606; ATCC) recognizes an epitope within the cell surface receptor binding domain of human fibronectin, and MC-480 (Developmental Studies Hybridoma Bank, Johns Hopkins University, Baltimore, Md.) recognizes stage-specific embryonic antigen 1 (SSEA-1), which is a developmentally regulated carbohydrate expressed on early mouse embryos and certain primitive human tumors. For analysis, cells were suspended in PBA (PBS with 1% BSA and 0.1% sodium azide) and incubated with primary antibody at 4°C for 30 min. After washing in PBA, cells were resuspended in phycoerythrin-conjugated goat anti-mouse immunoglobulin (TAGO; 1:80 in PBA). After an additional 30 min at 4°C, cells were washed and analyzed by using a FACStar flow cytometer (B-D Immunocytometry Systems). Median fluorescence intensity was determined by using Consort 30 software supplied with the instrument. Background fluorescence was determined for each cell type by reacting duplicate samples with the irrelevant P3X63Ag8 supernatant as the primary antibody.

Expression of neuronal cytoplasmic markers in transfected cells and single-cell subclones was evaluated by using an avidin-biotin-peroxidase detection system similar to that described above. Acetone-fixed cytopreps were prepared with 100,000 cells per slide. The primary antibodies used were murine monoclonal anti-secretogranin I (Boehringer Mannheim), rabbit polyclonal anti-neuron-specific enolase (anti-NSE; DAKO), and rabbit polyclonal anti-S-100 (DAKO).

Proliferation studies. Cells were harvested from subconfluent monolayers by trypsinization, washed once in PBS, and counted by hemacytometer in 0.2% trypan blue. Cells were then resuspended in complete medium without hygromycin B and dispensed into 24-well plates (Costar, Cambridge, Mass.) at 10,000 cells per well. Duplicate or triplicate wells were harvested by trypsinization on days 1, 3, 5, and 7, and viable cells were counted as described above. For thymidine incorporation studies, cells were collected and counted as described above but dispensed into 96-well plates at 2,000 cells per well. Triplicate wells were pulsed for 4 h with 0.5 μCi of ^{3}H-thymidine on days 1, 3, 5, and 7 postplating. Following the pulse, wells were harvested onto glass fiber filters by using a PHD (Cambridge, Mass.) cell harvester and counted by using standard liquid scintillation techniques on a Beckman LS 3801 apparatus.

Soft agar cloning studies. A 2.5-ml amount of molten 0.6% Sea-Kem agarose was added per well to six-well plates (Costar) and allowed to harden. Cells were harvested as described above and resuspended in complete medium at 4,000 cells per ml. An equal volume of 0.6% agarose was added, and 2.5 ml of the resultant suspension was overlayed in each of triplicate wells. Plates were then incubated at 37°C under 5% CO_2, and the number of macroscopic colonies per well was counted after 3 weeks.

Tumorigenicity studies. Control and transfected CHP-100 cultures were harvested as described above and resuspended at 75×10^6/ml in PBS without hygromycin. Six-week-old male athymic nude mice (Frederick Cancer Research Facility) maintained under clean conditions were inoculated subcutaneously with 100 μl of cell suspension in the right and left inguinal areas. Animals were sacrificed 11 to 18 days postinjection, and the well-encapsulated tumors were easily resected for weighing and then snap-freezing for frozen sectioning.

RESULTS

Cellular heterogeneity within CHP-100. We verified the existence of distinct morphologies within the N-*myc*-unamplified neuroepithelioma cell line CHP-100 by growing cells on chamber slides (Fig. 2A). Note the small, dense cells extending processes as they overlay the monolayer of large, flat cells with open nuclei. Interestingly, even in this normal-copy-number cell line, there appears to be differential N-*myc* expression in the two morphologic subtypes. N-*myc*-specific immunocytochemistry performed on a cytoprep prepared from a normal mixed culture shows that the small, neuritic cells stain darkly for N-*myc* protein, whereas most of the large, flat, and more open cells show only background staining (Fig. 2B). Note, however, the presence of occasional large cells that show N-*myc* positivity. The N-*myc*-

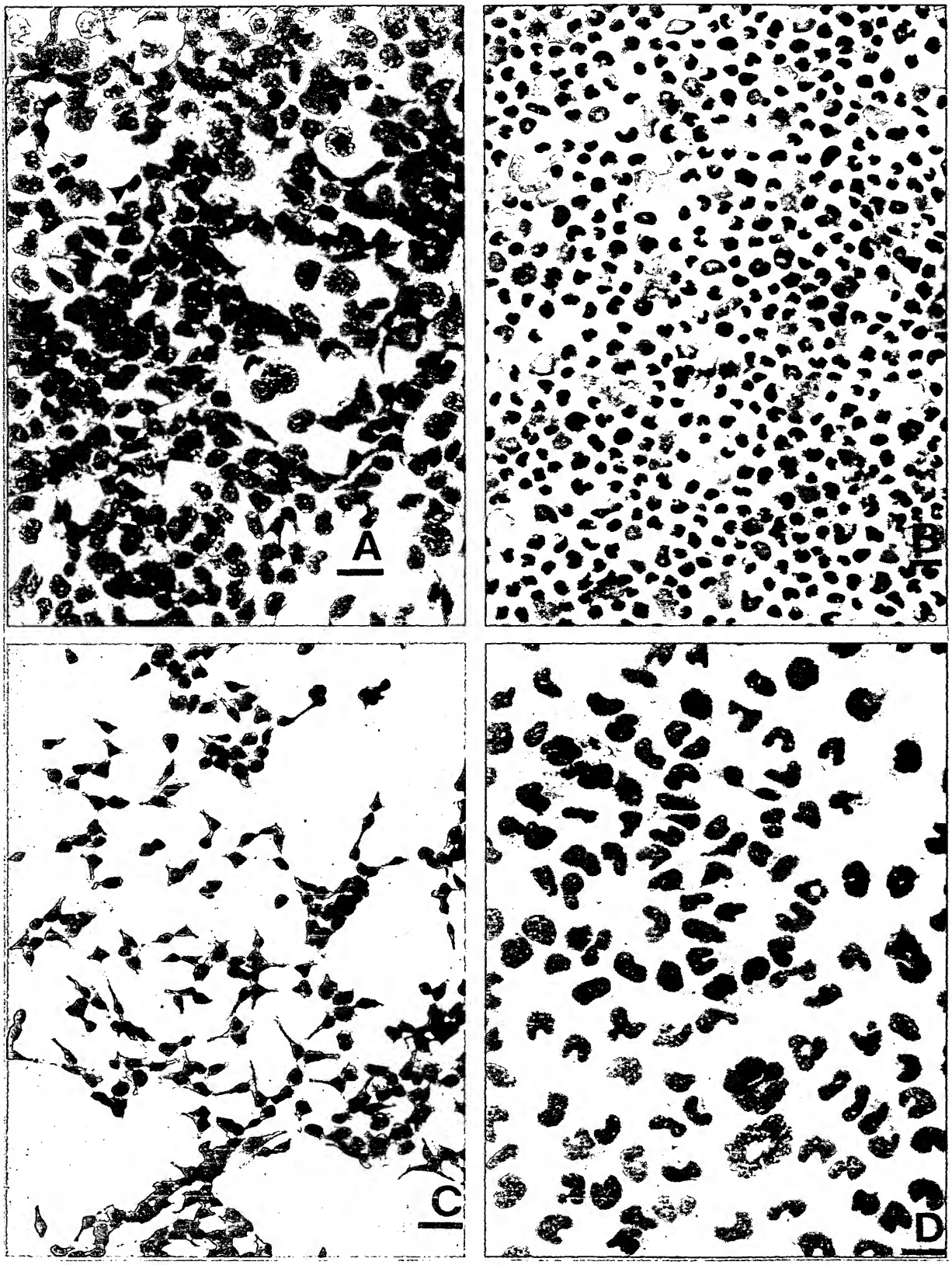

FIG. 2. Cellular heterogeneity in CHP-100. Cells were grown on a chamber slide and stained with the Diff-Quik kit (A). N-*myc*-specific immunocytochemistry with hematoxylin counterstain was performed on a cytoprep of a normal mixed culture (B). Chamber slide cultures of round and flat subclones were stained as in panel A (C and D, respectively). Bars = 20 μm.

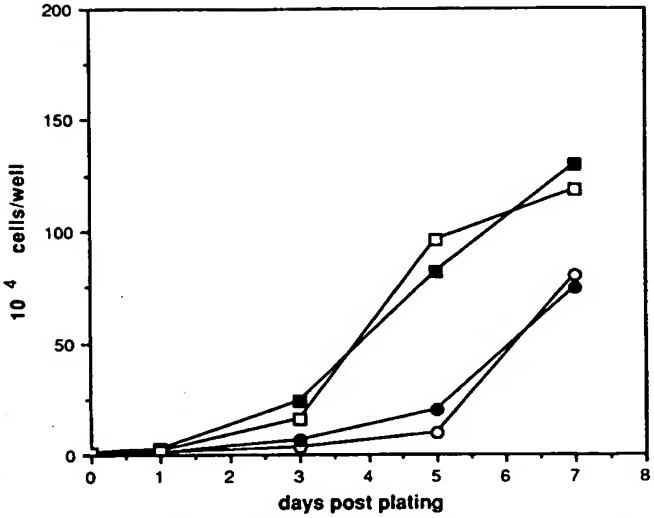

FIG. 3. Growth of mixed- versus single-phenotype CHP-100. Points represent means of triplicate wells initially seeded at 10^4 cells per well. Symbols: □, ■, independent mixed-type cultures; ○, flat subclone; ●, round subclone.

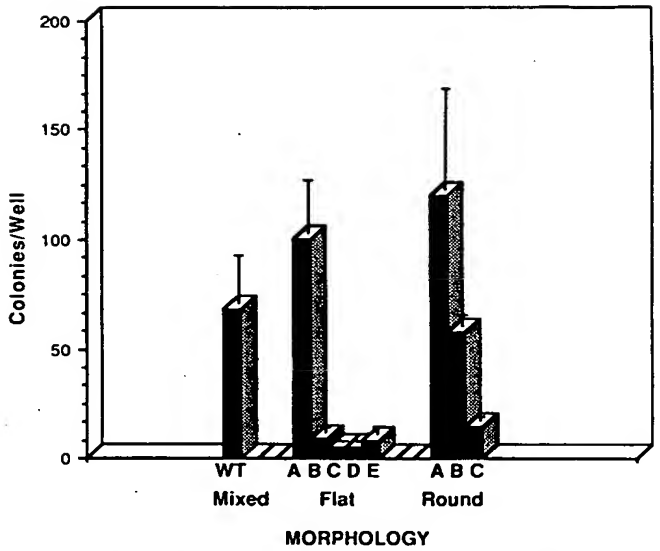

FIG. 4. Soft agar cloning of CHP-100 subclones. Each bar depicts an independently derived subclone of the morphology indicated. Data are expressed as means ± standard errors of triplicate wells.

amplified neuroblastoma line IMR-32 also showed variant morphologies in culture and a similar pattern of differential N-*myc* staining by immunocytochemistry (data not shown).

Single-cell subclones were isolated that maintained monotypic morphology over at least 12 passages in culture (Fig. 2C and D). Of note, these variant clones showed growth rates in monolayer culture significantly lower than those of wild-type, mixed-morphology cultures (Fig. 3). This finding may explain why mixed phenotypes are conserved in continuous culture without the overgrowth of one type over the other. The continued presence of both round and flat cells confers a clear growth advantage in monolayer culture. As reported for N-*myc*-amplified neuroblastoma variants, most round clones retain the ability to clone in soft agar, while most flat clones do not. Four of five randomly selected flat clones showed minimal ability to clone in soft agar (Fig. 4). Interestingly, unlike the other flat clones examined, the one flat clone showing marked clonagenicity (Flat/A) was unique in displaying clear N-*myc* reactivity (data not shown). The round clones examined demonstrated uniform N-*myc* reactivity but varying degrees of clonagenicity (Fig. 4). These data demonstrate that the morphologically variant subclones of CHP-100 display distinct functional characteristics as well.

An episomal antisense vector inhibits N-*myc* expression. As described in Materials and Methods, we constructed an episomal replicon designed to generate high levels of intranuclear antisense RNA to a portion of the N-*myc* genomic sequence. Sense and antisense vectors were electroporated into the highly N-*myc* amplified cell line IMR-32. After 4 weeks in selective antibiotic, duplicate cultures were set up from five independent clones for each vector type. Hygromycin was removed from the medium in one half the duplicates, and 10 days later cultures were examined for N-*myc* expression by immunoblotting. We observed marked diminution of N-*myc* signal in a representative antisense vector-transfected clone continued in hygromycin (Fig. 5B, lane 3). Lanes 1 and 2 show normal levels of N-*myc* signal in nontransfected and sense vector-transfected clones respectively, ruling out nonspecific effects of either our vector or hygromycin. There was diminution of N-*myc* in another antisense vector-carrying clone (Fig. 5C, lane 2), but when hygromycin was removed from this clone 10 days earlier as for lane 3 (allowing loss of vector), the signal returned to the level seen in sense vector-carrying clones continued in hygromycin (Fig. 5C, lanes 4 and 5). Recovery of expression indicates that transfection and selection alone did not result in N-*myc*-suppressed clones. In the control (Fig. 5A, lane 1),

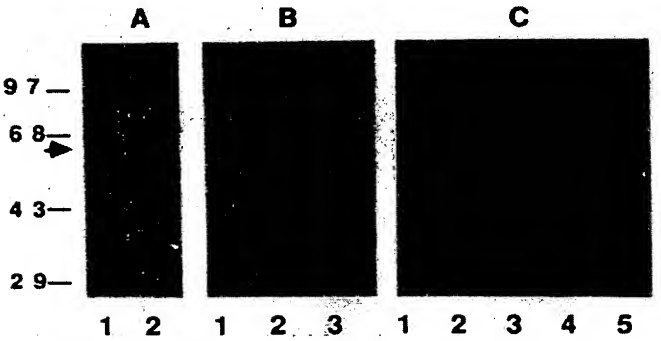

FIG. 5. Western blot analysis of N-*myc* in transfected IMR-32 clones. Total cellular protein (60 μg per lane) was fractionated on a 7% polyacrylamide gel and transferred to nitrocellulose. The relative level of N-*myc* protein expression was determined by using the N-*myc*-specific monoclonal antibody NMC II-100. (A) N-*myc*-nonexpressing, c-*myc*-overexpressing cell line HL-60 (lane 1) and prestained molecular weight markers (lane 2). (B) Nontransfected IMR-32 (lane 1), sense vector-transfected cells (lane 2), and antisense vector-transfected cells (lane 3). (C) Prestained markers (lane 1), antisense vector-transfected cells maintained in 200 μg of hygromycin B per ml (lane 2), antisense-transfected cells removed from hygromycin B 10 days prior to analysis (lane 3), and sense vector-transfected cells maintained in hygromycin B (lanes 4 and 5). Arrowhead indicates the location of N-*myc*-specific bands.

the absence of signal in c-*myc*-amplified HL-60 cells demonstrates the specificity of the N-*myc* antibody used.

N-*myc* suppression inhibits transdifferentiation. Figure 6 presents cytologic evidence demonstrating the morphologic correlates of N-*myc* suppression in a neuroblastoma cell line. In the sense vector-transfected cells (Fig. 6A), note the numerous small, darkly staining cells surrounding the larger, more open cells. In Fig. 6B, note the almost complete absence of these smaller cells in an antisense vector-transfected clone. Immunocytochemical analysis of the antisense vector-transfected clone demonstrates a marked loss of N-*myc* reactivity (data not shown), as would be predicted from the Western blot data discussed above (Fig. 5). Figure 6C demonstrates the exuberant recovery of mixed morphology after removal of hygromycin 10 days earlier from the clone shown in Fig. 6B.

Because we were not able to document N-*myc* expression by immunoblot in CHP-100, we confirmed the existence of low-level N-*myc* expression at the RNA level by poly(A) Northern (RNA) analysis and reverse transcriptase polymerase chain reaction in control experiments (22). For subsequent vector experiments, we relied on immunocytochemistry to assess N-*myc* expression at the protein level in transfected CHP-100 cells. Similar to the results shown above for IMR-32, Fig. 7 demonstrates the effects of vector transfection on both morphology and N-*myc* expression in CHP-100. Antisense vector-transfected cells maintained in hygromycin (Fig. 7C) show reduced N-*myc*-specific staining, while sense vector-transfected cells (Fig. 7A) and antisense vector-transfected cells from which hygromycin was previously removed (Fig. 7B) show easily detected staining. Morphologic effects are also clearly seen. Only the antisense vector-transfected culture maintained in hygromycin shows loss of small, neuritic cells.

Phenotypic characterization of CHP-100 single-cell clones and N-*myc*-suppressed clones. To better characterize the morphologically monotypic, single-cell-derived CHP-100 subclones, we analyzed the expression of several neural antigens. Table 1 depicts the pattern of neural marker expression detected on a panel of randomly selected flat and round subclones. All clones are strongly positive for S-100 protein, supporting their origin from the same common neuroectodermal antecedent. Expression of NSE and secretogranin I, however, is restricted to round subclones and, within a mixed-morphology wild-type culture, to cells of small, round phenotype. The round clone F, which does not express NSE or secretogranin I, is unusual in that it also clones poorly in soft agar (Fig. 4, Round/C).

Sense vector-transfected CHP-100 clones such as D5+ (Table 1) express neural markers as expected and display mixed morphology, while antisense vector-transfected, N-*myc*-suppressed cells (B2+; Table 1) lose expression of NSE and secretogranin I. Most importantly, when hygromycin is removed from the culture, resulting in recovery of N-*myc* expression, neural marker expression also returns (B2−; Table 1), ruling out the possibility that lack of marker expression was simply a peculiarity of the particular clone examined. All of the individually isolated antisense vector-transfected clones were similar in morphology and neural antigen expression to the B2 clone described in Table 1 (data not shown). These data emphasize the value of an episome-generated antisense approach to studying gene expression in heterogeneous cell populations, such as exist in neuroblastoma and neuroepithelioma cell lines.

In addition to the neural antigens described above, expression of the important cell adhesion-communication molecular fibronectin is modulated either directly or indirectly by N-*myc* (Table 2). Inhibition of N-*myc* expression leads to a reproducible decline in surface-associated fibronectin expression. This decrease is not due to a simple toxic effect of hygromycin, since sense vector-transfected cells maintained in the drug display normal levels of fibronectin. Additionally, this effect is reproducibly observed in individually isolated antisense vector-transfected clones. Table 2 also demonstrates an inverse relationship between N-*myc* expression and expression of the early embryonic antigen SSEA-1. N-*myc*-suppressed clones show higher levels of SSEA-1 than do their nonsuppressed counterparts. These data suggest that the presence of episomal replicons is not inducing a general decline in protein synthesis. While neural marker and fibronectin expression decline in the presence of an antisense-generating vector, SSEA-1 expression actually rises. Hygromycin alone is not inducing SSEA-1, as a sense vector-transfected clone maintained in hygromycin remains negative for this antigen (Table 2).

Using simultaneous dual-parameter flow cytometric analysis, we examined the coexpression on individual cells of the antigens Leu 7 and fibronectin (Fig. 8). In such an analysis, the number of cells in a population carrying one, both, or neither of the markers being examined can be seen. The flat cells (Fig. 8D) demonstrate marked fibronectin and Leu 7 positivity, while round cells (Fig. 8C) are fibronectin negative and Leu 7 intermediate. The mixed, wild-type culture (Fig. 8A) shows the presence of both cell surface phenotypes, as would be expected. N-*myc*-suppressed cells possess a surface phenotype characteristic of neither flat nor round clones (Fig. 8B). These data are consistent in the other flat, round, and antisense vector-transfected clones examined and further demonstrate that the morphologically characterized flat and round cell clones display distinct antigenic profiles. In addition, these data demonstrate that, together with the morphologic alterations described above, N-*myc* suppression results in quantifiable changes in several differentiation-modulated cytoplasmic and surface antigenic determinants.

N-*myc* suppression and growth. As noted above, single-cell cloning experiments with CHP-100 demonstrated that normal mixed cultures of flat and round cells grow more rapidly in monolayer culture than do either monotypic flat or round clones (Fig. 3). If inhibition of N-*myc* expression blocks the development of mature round or flat cells in culture, antisense vector-carrying cultures should proliferate more slowly. Figure 9 depicts thymidine incorporation over time for nontransfected, wild-type cells as well as antisense vector-carrying cells (confirmed by immunocytochemistry to be N-*myc* suppressed) and antisense vector-carrying cells removed from hygromycin 2 weeks earlier (N-*myc* present by immunocytochemistry). N-*myc* suppression clearly decreases but does not totally block DNA synthesis. Although we cannot say that N-*myc* expression is totally inhibited (because of the limitations of the technique that we have used to measure it), significant suppression by the vector does not result in either cell death or terminal differentiation but rather results in a decrease of proliferative rate. This decrease in growth rate is not due to cross-inhibition by the vector of c-*myc* expression. Figure 10 demonstrates by immunoblot analysis that levels of c-*myc* expression are similar in sense, antisense, and control vector-transfected cells as well as nontransfected cells. IMR-32 (which does not express c-*myc* but does express high levels of N-*myc*) serves as a negative control in the first lane and demonstrates the specificity of the c-*myc* antibody used.

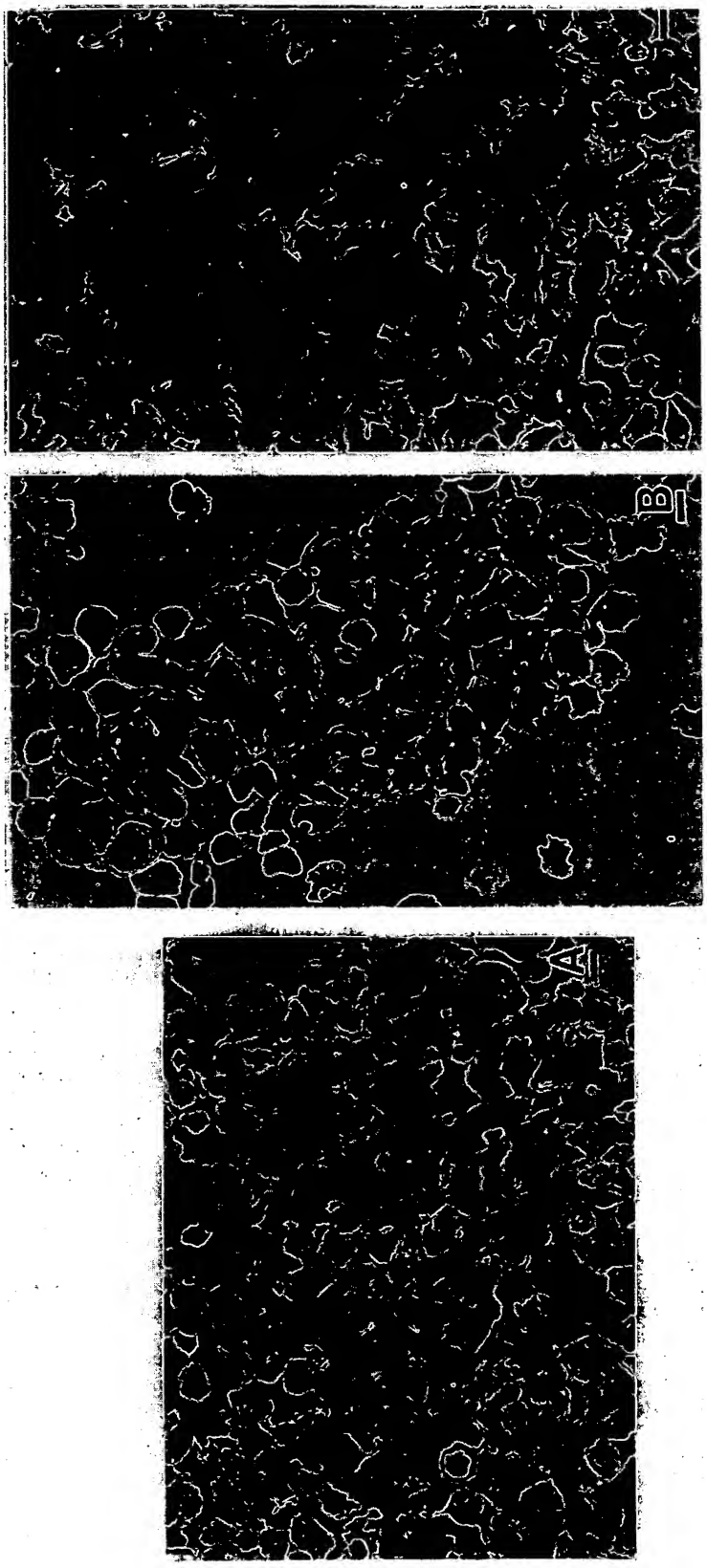

FIG. 6. Cytology of transfected IMR-32 cells. Cytopreps were made 40 days after transfection and stained with the Diff-Quik kit. (A) Sense vector transfectants; (B) antisense vector transfectants; (C) antisense vector transfectants removed from hygromycin B 10 days prior to analysis. Bars = 30 μm.

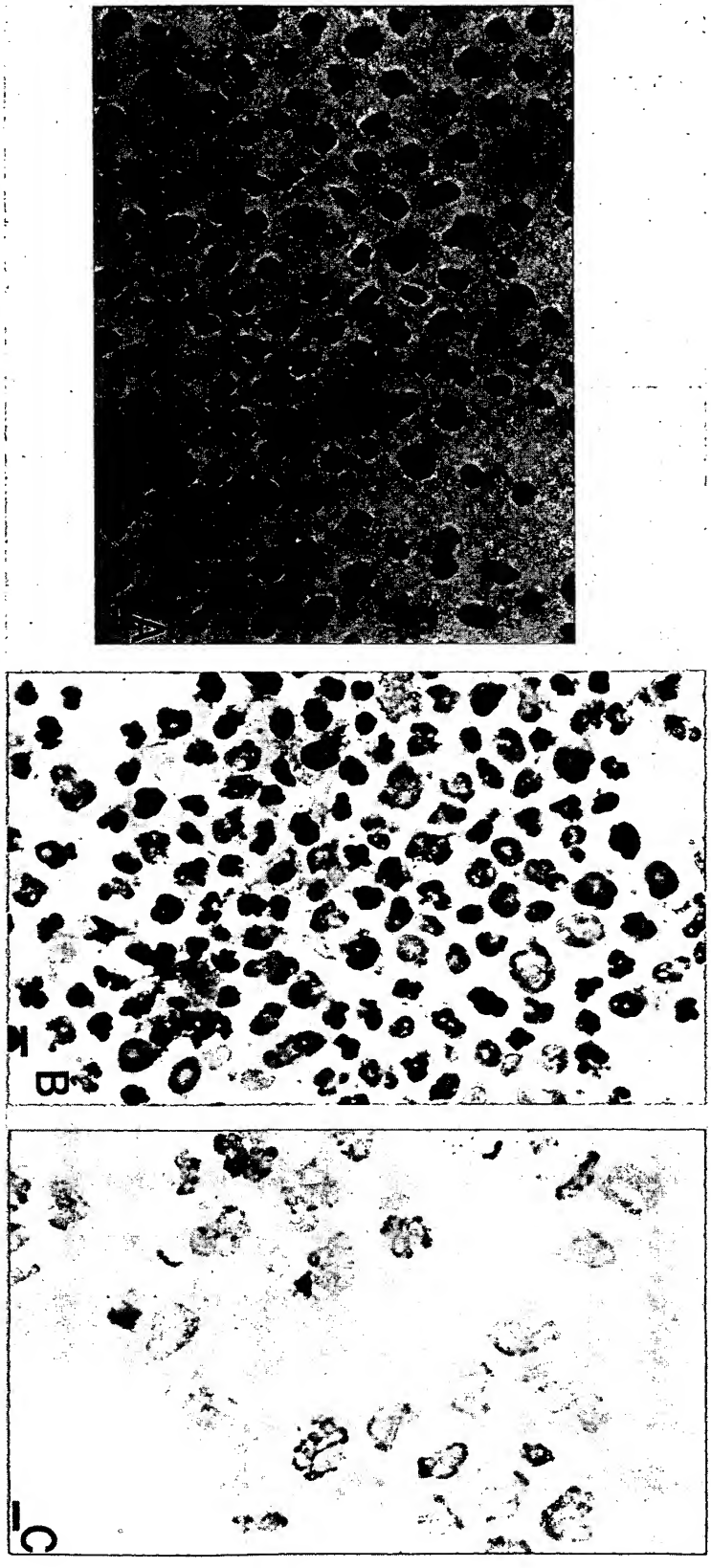

FIG. 7. Immunocytology of transfected CHP-100. Cytopreps were made 50 days following transfection, fixed, and reacted with an N-*myc*-specific monoclonal antibody to demonstrate both morphology and relative levels of N-*myc* expression. (A) Sense vector transfectants; (B) antisense vector transfectants removed from hygromycin 14 days prior to analysis; (C) antisense vector transfectants maintained in hygromycin B. Bars = 30 μm.

TABLE 1. Expression of neural markers by CHP-100 subclones and vector transfectants[a]

Clone	Morphology	Reactivity[b]		
		Secretogranin I	NSE	S-100
Wild type	Mixed	+	+	+
A	Flat	−	−	+
B	Flat	−	−	+
C	Flat	−	−	+
D	Flat	−	−	+
E	Flat	−	−	+
F	Round	−	−	+
B3	Round	+	+	+
C3	Round	+	+	+
D5+[c]	Mixed	+	+	+
B2+[d]	Flat	−	−	+
B2−[e]	Mixed	+	+	+

[a] Acetone-fixed cytopreps were prepared with 100,000 cells per slide and stained by an indirect immunoperoxidase technique.
[b] +, >15% of at least 300 cells examined showed clear immunoreactivity compared with control antibody; −, no reactivity.
[c] CHP-100 clone transfected with N-*myc* sense-generating vector and maintained in hygromycin.
[d] CHP-100 clone transfected with N-*myc* antisense-generating vector and maintained in hygromycin.
[e] CHP-100 clone removed from hygromycin 3 weeks prior to staining.

To determine whether the decrease in proliferative rate of N-*myc*-suppressed CHP-100 correlates with in vivo tumorigenicity, transfected, N-*myc*-suppressed or nonsuppressed cells were injected into nude mice (in the absence of hygromycin), and the resultant tumor mass was measured after three different time intervals. Figure 11 demonstrates a decrease in the average size of tumors produced by antisense vector-carrying cells compared with cells grown without hygromycin for 2 weeks prior to injection. N-*myc*-suppressed cells, however, clearly produce tumors. The difference in tumor size between antisense-expressing and -nonexpressing groups is significant only for days 11 and 14 ($P = 0.056$).

DISCUSSION

Although by no means fully understood, the transdifferentiation process commonly observed in pediatric neuroectoderm-derived tumors provides an opportunity to study the role of genes regulating tissue-specific growth or differentiation. Because we and others (16, 22) have observed that N-*myc* is generally expressed in round but not flat cells in culture, we reasoned that N-*myc* expression may play a role in regulating transdifferentiation. Although a fully developed paradigm of well-characterized developmental stages for CHP-100 is beyond the scope of this report, our results do indicate that N-*myc* expression is clearly required for transdifferentiation in vitro.

TABLE 2. Modulation by N-*myc* antisense RNA of expression of cell surface markers in CHP-100

Cell type	Fluorescence intensity[a]						
	Expt 1, HFN	Expt 2		Expt 3		Expt 4	
		HFN	SSEA-1	HFN	SSEA-1	HFN	SSEA-1
Antisense, vector transfected							
+Hygromycin	2	3	3	1	6	3	28
−Hygromycin	12	8	0	13	0	12	10
Sense, vector transfected							
+Hygromycin	9					15	0

[a] Expressed as median fluorescence intensities (in arbitrary units) of a population of 3,000 cells per data point as determined by flow cytometric analysis. Experiments 1, 2, and 3 were performed by using the same clones on different occasions. Experiment 4 was performed with different clones derived from an independent transfection. HFN, Human fibronectin.

We have characterized individually isolated flat and round cell clones obtained from CHP-100 wild-type cultures. Not only are these clones morphologically monomorphic (i.e., 100% flat or round), but they express unique phenotypic and functional attributes as well. Thus, flat cell isolates do not clone in soft agar (four of five; Fig. 4), do not express the neural antigen secretogranin I or NSE (five of five; Table 1), and express high levels of fibronectin and Leu 7 (Fig. 8). Conversely, round cell isolates clone to a variable extent in soft agar (three of three; Fig. 4), express secretogranin and NSE (two of three; Table 1), but do not express fibronectin and express Leu 7 at lower intensity (Fig. 8). As expected, wild-type cultures display mixed expression of these characteristics, and all clones, irrespective of morphologic type, express the neuroectoderm specific antigen S-100.

Inhibition of N-*myc* expression prevents development of the neuronal phenotype as characterized in CHP-100 by round shape and positivity for NSE and secretogranin I (Table 1). Although morphologically similar, N-*myc*-inhibited cells are also distinct from clonally derived flat cells. They rapidly revert to mixed phenotype upon loss of the N-*myc* block (Fig. 7), continue to be tumorigenic in nude mice (Fig. 11), and clone in soft agar (data not shown). In addition, they express low levels of fibronectin characteristic of round cells while continuing to express levels of Leu 7 characteristic of flat cells (15, 23; Fig. 8). Cells with this same pattern of fibronectin and Leu 7 expression are detectable in wild-type cultures (Fig. 8A, quadrant 4), but to date we have been unable to isolate phenotypically pure clones. Given that they express phenotypic and functional characteristic of both flat and round cells, N-*myc*-suppressed cells may in fact represent intermediate cells in a continuum of transdifferentiating phenotypes, as recently described by Ciccarrone et al. in neuroblastoma cell lines (4). The finding that SSEA-1 reactivity is increased following N-*myc* suppression also supports the concept of a block to differentiation (Table 2), since this early embryonic antigen is not expressed on more mature cell types, and the related antigen SSEA-3 is known to be down-regulated during the retinoic acid-induced differentiation of multipotent teratocarcinoma cell lines (2).

Although N-*myc*-suppressed cells are phenotypically and morphologically monomorphic and are distinct from either flat or round cell clones, removal of the antisense block leads to a rapid reappearance of both phenotypic and morphologic heterogeneity characteristic of wild-type cultures. The hypothesis that N-*myc* suppression inhibits transdifferentiation implies that the occasional large, N-*myc*-positive cell seen in wild-type cultures (Fig. 2B) actually represents an intermediate cell and raises the intriguing possibility that transient N-*myc* expression in an intermediate type cell is required to generate both N-*myc*-negative flat cells and N-*myc*-positive round cells.

The finding that N-*myc* down-regulation precedes retinoic acid-induced differentiation in certain cell lines (11, 28) does not conflict with the data presented here. Our results make it clear that down-regulation of N-*myc*, while probably necessary for terminal neuritic differentiation, is not sufficient to

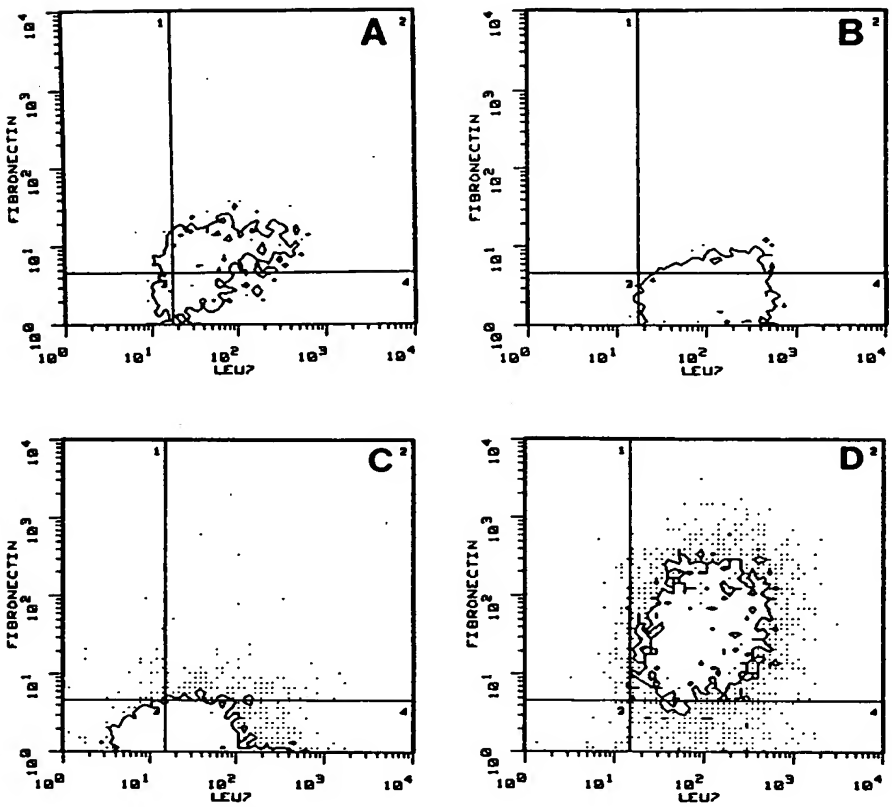

FIG. 8. Dual-parameter flow cytometric analysis of CHP-100 and subclones. Cells were incubated with monoclonal antibody HFN 7.1 (antifibronectin), followed by phycoerythrin-conjugated goat anti-mouse immunoglobulin and then fluorescein isothiocyanate-conjugated Leu 7. The *x* axis represents Leu 7 fluorescence, and the *y* axis represents fibronectin fluorescence. Fluorescence intensities are displayed on log axes; box 3 in each panel contains dual-negative cells, and box 2 contains dual-positive cells; box 1 contains only fibronectin-positive cells, and box 4 contains only Leu 7-positive cells. The contours depict relative cell number. (A) Normal, mixed culture; (B) antisense vector-transfected, N-*myc*-suppressed clone; (C) round subclone; (D) flat subclone.

initiate this process. IMR-32 cells, which are known to differentiate in response to retinoic acid, did not show neuritic morphologic differentiation despite marked inhibition of N-*myc* expression by vector-generated antisense RNA. Terminal differentiation of a mixed-phenotype culture may require N-*myc* down-regulation in N-type cells. Generation of these N-type cells in the first place, however, may well require at least transient N-*myc* expression. Such a requirement for transient expression could mirror the normal pattern of N-*myc* expression seen in several organ systems during fetal development. It will be informative to determine whether retinoic acid is still able to induce neuritic differentiation in vector-carrying, N-*myc*-suppressed neuroblastoma cells. If N-*myc* suppression does result in freezing cells in an intermediate or I-type state (where they continue to be tumorigenic), they may not be able to respond to the differentiating effects of agents like retinoic acid. Such a finding could also have important negative implications if one contemplates N-*myc* as a potential target for antioncogene therapy.

In CHP-100, N-*myc* suppression clearly leads to slower growth in vitro and probably in vivo. Although we cannot rule out a direct role in control of proliferation, the lack of effect of N-*myc* suppression on c-*myc* levels makes this an unlikely possibility. Instead, N-*myc* suppression could easily slow growth solely as a result of its inhibition of the transdifferentiation process. As suggested by Finklestein and Weinberg (6) in their work on retinoid-induced differentiation of teratocarcinoma, c-*myc* may play a direct role in growth control while N-*myc* is more involved in regulating differentiative processes. This explanation would correlate well with the clinical finding that N-*myc* amplification is associated with aggressive, poor-prognosis neuroblastoma but is rarely seen in low-stage disease (21, 27). If N-*myc* expression is rate limiting to the transdifferentiation process, amplification would favor more rapid growth and also the accumulation of independently tumorigenic, potentially more metastatic N-type cells.

Although N-*myc* suppression does not prevent tumor growth in nude mice, tumor size is significantly reduced 11 and 14 days after injection. Dilutional loss of vector due to growth in the mouse without selective pressure from hygromycin may account for the smaller difference between groups by day 18. We hope to develop a method for N-*myc* staining of frozen sections, in which case tumors resected at day 18 should show a return to more normal levels of N-*myc* expression if the hypothesis presented above is correct. Although the argument could be made that tumor growth occurred in our system because of inadequate N-*myc* suppression, this possibility seems unlikely in that our episomal vector was able to markedly suppress N-*myc* expression in the highly N-*myc* amplified cell line IMR-32. Inhibition in the

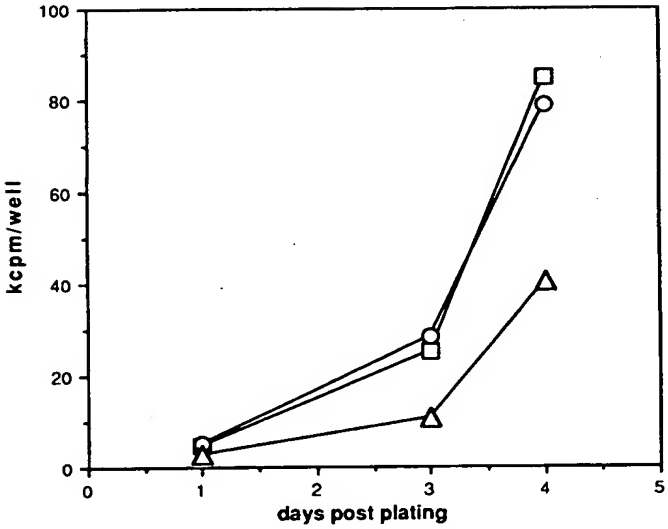

FIG. 9. DNA synthesis by N-*myc*-suppressed CHP-100. A total of 2,000 cells per well were plated in 96-well plates on day 0. Triplicate wells were pulsed with 0.5 μCi of ^{3}H-thymidine on the days indicated. Symbols: □, normal wild-type cultures; ○, antisense vector-transfected cells removed from hygromycin B 14 days prior to the experiment (N-*myc* nonsuppressed); △, antisense vector transfectants maintained in hygromycin until the day of the experiment (N-*myc* suppressed).

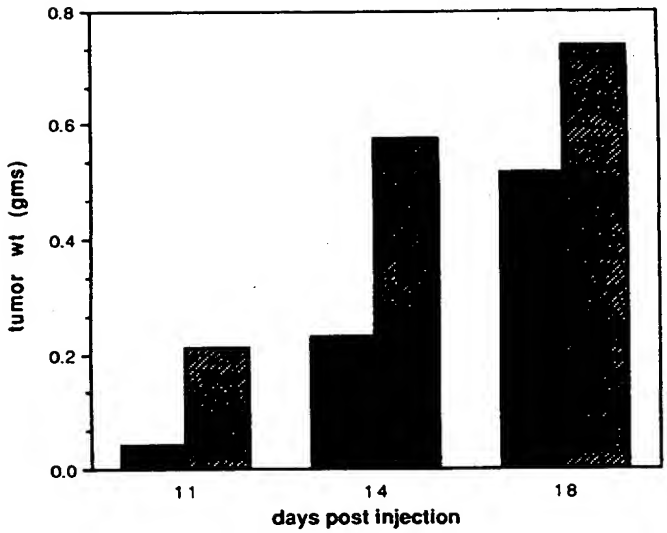

FIG. 11. Tumorigenicity of transfected CHP-100 cells. Nude mice were injected subcutaneously with 10^7 cells. In independent experiments, mice were sacrificed on day 11, 14, or 18 postinjection. The well-encapsulated tumors were excised and weighed. Solid bars depict the mean weights of tumors produced by antisense vector-transfected cells maintained in hygromycin until the day of injection; hatched bars represent the mean weights of tumors produced by the same clone removed from hygromycin 14 days prior to injection.

much lower expressing CHP-100 line should have been nearly complete. Regardless of these considerations, the data show that low-level N-*myc* expression in an N-*myc*-nonamplified cell line probably increases tumor growth rate but certainly is not essential for tumorigenicity. This finding is not surprising, since many previous reports have documented that N-*myc* alone does not transform cells but must cooperate with another activated oncogene, such as *ras*, to bring about the malignant phenotype (30). Indeed, as previously noted (6), although N- and c-*myc* display similar properties in transformation assays, there is much evidence to suggest they have different roles in the regulation of gene expression.

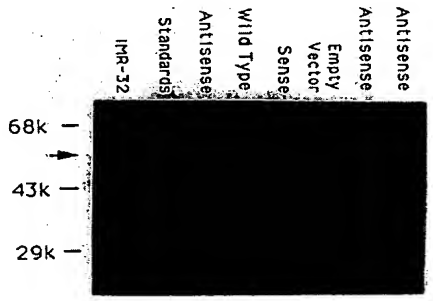

FIG. 10. Western blot analysis of c-*myc* in transfected CHP-100. Total cellular protein (60 μg per lane) was fractionated on a 7% polyacrylamide gel and transferred to nitrocellulose. The relative level of c-*myc* expression was determined by using the c-*myc*-specific monoclonal antibody MYC CT14-G4.3. The left-most lane demonstrates nonreactivity of the antibody with a lysate prepared from N-*myc*-amplified but c-*myc*-nonexpressing IMR-32 cells; the second lane contains prestained molecular weight markers. Sense and antisense lanes depict c-*myc* levels in independent CHP-100 clones carrying the respective vectors. The wild-type lane contains lysate from nontransfected CHP-100 cells, while the empty vector lane contains lysate from a CHP-100 clone transfected with vector generating neither sense nor antisense RNA to N-*myc*. Arrowhead depicts location of c-*myc*-specific bands. k, Kilodaltons.

In summary, we have shown for the first time that an antisense RNA-generating episomal replicon can be used to effectively suppress even highly amplified oncogene expression. Without decreasing c-*myc* expression, N-*myc* suppression leads to inhibition of phenotypic and morphologic transdifferentiation, with subsequent effects on growth in human neuroectoderm-derived cell lines. Our results specifically implicate N-*myc* in maintaining the cellular heterogeneity commonly observed in these tumors in vitro. Finally, the technique reported should be quite useful in studying any proto-oncogene whose overexpression plays a role in the molecular basis of a particular tumor's biology.

ACKNOWLEDGMENTS

We thank M. Tykocinski, Case Western Reserve University, for the generous gift of plasmid pREP3 and for helpful discussions regarding its use. We thank N. Ikegaki and R. H. Kennett, University of Pennsylvania, for the generous gift of N-*myc*-specific hybridoma supernatant and Rick Dreyfuss, NIH Photomicrography, for technical assistance. The hybridoma MC-480 was obtained from the Developmental Studies Hybridoma Bank maintained by the Department of Pharmacology and Molecular Sciences, John Hopkins University School of Medicine, Baltimore, Md., and the Department of Biology, University of Iowa, Iowa City, under contract N01-HD-6-2915 from NICHD.

REFERENCES

1. **Akeson, R., and R. Bernards.** 1990. N-*myc* down regulates neural cell adhesion molecule expression in rat neuroblastoma. Mol. Cell. Biol. **10**:2012–2016.
2. **Andrews, P. W.** 1984. Retinoic acid induces neuronal differen-

tiation of a cloned human embryonal carcinoma cell line in vitro. Dev. Biol. 103:285–293.
3. **Charron, J., B. A. Malynn, E. J. Robertson, S. P. Goff, and F. W. Alt.** 1990. High frequency disruption of the N-myc gene in embryonic stem and pre-B cell lines by homologous recombination. Mol. Cell. Biol. 10:1799–1804.
4. **Ciccarone, V. C., B. A. Spengler, M. B. Meyers, J. L. Biedler, and R. A. Ross.** 1989. Phenotypic diversification in human neuroblastoma cells: expression of distinct neural crest lineages. Cancer Res. 49:219–225.
5. **Collum, R. G., and F. W. Alt.** 1990. Are myc proteins transcription factors? Cancer Cells 2:69–75.
6. **Finklestein, R., and R. Weinberg.** 1988. Differential regulation of N-myc and c-myc expression in F9 teratocarcinoma cells. Oncogene Res. 3:287–292.
7. **Groger, R. K., D. M. Morrow, and M. L. Tykocinski.** 1989. Directional antisense and sense cDNA cloning using Epstein-Barr virus episomal expression vectors. Gene 81:285–294.
8. **Hambor, J. E., C. A. Hauer, H. Shu, R. K. Groger, D. R. Kaplan, and M. L. Tykocinski.** 1988. Use of an Epstein-Barr virus episomal replicon for antisense RNA-mediated gene inhibition in a human cytotoxic T-cell clone. Proc. Natl. Acad. Sci. USA 85:4010–4014.
9. **Holt, J. T., T. V. Gopal, A. D. Moulton, and A. W. Nienhuis.** 1986. Inducible production of c-fos antisense RNA inhibits 3T3 cell proliferation. Proc. Natl. Acad. Sci. USA 83:4794–4798.
10. **Ikegaki, N., J. Bukovsky, and R. H. Kennett.** 1986. Identification and characterization of the N-myc gene product in human neuroblastoma cells by monoclonal antibodies with defined specificities. Proc. Natl. Acad. Sci. USA 83:5929–5933.
11. **Kato, K., A. Kanamori, and H. Kondoh.** 1990. Rapid and transient decrease of N-myc expression in retinoic acid-induced differentiation of OTF9 teratocarcinoma stem cells. Mol. Cell. Biol. 10:486–491.
12. **Kohl, N. E., N. Kanda, R. R. Schreck, G. Bruns, S. A. Latt, F. Gilbert, and F. W. Alt.** 1983. Transposition and amplification of oncogene related sequences in human neuroblastomas. Cell 35:359–367.
13. **Lee, W., A. L. Murphree, and W. F. Benedict.** 1984. Expression and amplification of the N-myc gene in primary retinoblastoma. Nature (London) 309:458–460.
14. **Lutfalla, G., L. Armbruster, S. Dequin, and R. Bertolotti.** 1989. Construction of an EBNA-producing line of well-differentiated hepatoma cells and of appropriate Epstein-Barr virus-based shuttle vectors. Gene 76:27–39.14.
15. **Matsumura, T., T. Sugimoto, and T. Sawada.** 1988. Phenotypes of neuroblastoma cells as distinguished by monoclonal antibodies, p. 38–55. *In* M. Sluyser and P. A. Voute (ed.), Molecular biology and genetics of childhood cancers: approaches to neuroblastoma. Ellis Horwood Limited, Chichester, West Sussex, England.
16. **Michitsch, R. W., J. L. Biedler, and P. W. Melera.** 1988. Modulation of N-myc expression, but not tumorigenicity accompanies phenotypic conversion of neuroblastoma cells in prolonged culture, p. 103–120. *In* A. E. Evans, G. J. D'Angio, A. G. Knudson, and R. C. Seeger (ed.), Advances in neuroblastoma research 2. Alan R. Liss, New York.
17. **Mugrauer, G., F. W. Alt, and P. Ekblom.** 1988. N-*myc* proto-oncogene expression during embryogenesis in the developing mouse as revealed by in situ hybridization. J. Cell Biol. 107: 1325–1335.
18. **Nakajima, H., M. Ikeda, N. Tsuchida, S. Nishimura, and Y. Taya.** 1989. Inactivation of the N-myc gene product by single amino acid substitution of leucine residues located in the leucine-zipper region. Oncogene 4:999–1002.
19. **Nau, M. M., B. J. Brooks, D. N. Carney, A. F. Gazdar, J. F. Battey, E. A. Sausville, and J. D. Minna.** 1986. Human small-cell lung cancers show amplification and expression of the N-myc gene. Proc. Natl. Acad. Sci. USA 83:1092–1096.
20. **Rettig, W. J., B. A. Spengler, P. G. Chesa, L. J. Old, and J. L. Biedler.** 1987. Coordinate changes in neuronal phenotype and surface antigen expression in human neuroblastoma cell variants. Cancer Res. 47:1383–1389.
21. **Rosen, N., C. P. Reynolds, C. J. Thiele, J. L. Biedler, and M. A. Israel.** 1986. Increased N-myc expression following progressive growth of human neuroblastoma. Cancer Res. 46:4139–4142.
22. **Rosolen, A., L. Whitesell, N. Ikegaki, R. H. Kennett, and L. M. Neckers.** 1990. Antisense inhibition of single copy N-myc expression results in decreased cell growth without reduction of c-myc protein in a neuroepithelioma cell line. Cancer Res. 50:6316–6322.
23. **Ross, R. A., V. Ciccarone, M. B. Meyers, B. A. Spengler, and J. L. Biedler.** 1988. Differential expression of intermediate filaments and fibronectin in human neuroblastoma cells, p. 277–289. *In* A. E. Evans, G. J. D'Angio, A. G. Knudson, and R. C. Seeger (ed.), Advances in neuroblastoma research 2. Alan R. Liss, New York.
24. **Ross, R. A., B. A. Spengler, and J. L. Biedler.** 1983. Coordinate morphological and biochemical interconversion of human neuroblastoma cells. J. Natl. Cancer Inst. 71:741–747.
25. **Schlesinger, H. R., J. M. Gerson, P. S. Moorhead, H. Maguire, and K. Hummeler.** 1976. Establishment and characterization of human neuroblastoma cell lines. Cancer Res. 36:3094–3100.
26. **Schwab, M., K. Alitalo, K. Klempnauer, H. E. Varmus, J. M. Bishop, F. Gilbert, G. Brodeur, M. Goldstein, and J. Trent.** 1983. Amplified DNA with limited homology to myc cellular oncogene is shared by human neuroblastoma cell lines and a neuroblastoma tumor. Nature (London) 305:245–248.
27. **Seeger, R. C., G. M. Brodeur, H. Sather, A. Dalton, S. E. Siegel, K. Y. Wong, and D. Hammond.** 1985. Association of multiple copies of the N-myc oncogene with rapid progression of neuroblastomas. N. Engl. J. Med. 313:1111–1116.
28. **Thiele, C. J., C. P. Reynolds, and M. A. Israel.** 1985. Decreased expression of N-myc precedes retinoic acid-induced morphological differentiation of human neuroblastoma. Nature (London) 313:404–406.
29. **Tumilowicz, J. J., W. W. Nichols, J. J. Cholon, and A. E. Greene.** 1970. Definition of a continuous human cell line derived from neuroblastoma. Cancer Res. 30:2110–2118.
30. **Yancopoulos, G. D., P. D. Nissen, A. Tesfaye, N. E. Kohl, M. P. Goldfarb, and F. W. Alt.** 1985. N-myc can cooperate with ras to transform normal cells in culture. Proc. Natl. Acad. Sci. USA 82:5455–5459.
31. **Yates, J. L., N. Warren, and W. Sugden.** 1985. Stable replication of plasmids derived from Epstein-Barr virus in various mammalian cells. Nature (London) 313:812–815.
32. **Zimmerman, K. A., G. D. Yancopoulos, R. G. Collum, R. K. Smith, N. E. Kohl, K. A. Denis, M. M. Nau, O. N. Witte, D. Toran-Allerand, C. E. Gee, J. D. Minna, and F. W. Alt.** 1986. Differential expression of myc family genes during murine development. Nature (London) 319:780–783.